BRNO UNIVERSITY OF TECHNOLOGY
VYSOKÉ UČENÍ TECHNICKÉ V BRNĚ

FACULTY OF CIVIL ENGINEERING
FAKULTA STAVEBNÍ

INSTITUTE OF STRUCTURAL MECHANICS
ÚSTAV STAVEBNÍ MECHANIKY

ALGORITHMS FOR DESIGN AND ANALYSIS OF MEMBRANE STRUCTURES

ALGORITMY PRO NÁVRH A ANALÝZU MEMBRÁNOVÝCH KONSTRUKCÍ

DOCTORAL THESIS
DISERTAČNÍ PRÁCE

AUTHOR — M.Eng. Ing. Rostislav Lang
AUTOR PRÁCE

SUPERVISOR — doc. Ing. IVAN NĚMEC, CSc.
VEDOUCÍ PRÁCE

BRNO 2019

BIBLIOGRAFIC CITATION

LANG, Rostislav. *Algorithms for design and analysis of membrane structures.* Brno, 2019. 139 p. Doctoral thesis. Brno University of Technology, Faculty Civil Engineering, Department of Structural Mechanics. Supervised by doc. Ing. Ivan Němec, CSc.

CONTENT

1 INTRODUCTION

The membrane structures are fascinating from many points of view. From an architectural aspect, they are light, beautiful and non-conventional. From a civil engineer's point of view, membrane structures have the ability to overcome large spans and are really uncommon in their design and fabrication processes, both of them influenced by special requirements associated with these structures. From a point of view of a developer of a computer FEM software, these structures represent a great challenge, as it is necessary to cope with their large nonlinearities in structural analysis, and develop special tools for form finding and cutting pattern generation. More than anywhere else, the cooperation of all these professions can be observed as the shapes of tensile structures are driven by the will of nature and its physical laws more than by the will of a man.

Fig. 1 Iconic Structure Tanzbrunnen Designed by Frei Otto, Cologne, Germany [I, II]

Fig. 2 Roof of Denver International Airport, USA [III]

These structures are able to take impressive shapes and to overcome large spans, so they are used for roofing of public spaces (Fig. 1), stadiums, stations, airports (Fig. *2*), etc.

1.1 OUTLINE OF THESIS

This thesis is structured into the following chapters, covering the particular design steps of membrane structures.

Form Finding

Membrane structures are made of the material that only acts in tension and, as a consequence of this fact, the structural response of them is derived from their tension and curvature. For these structures, the statement 'Form follows force' is completely true, therefore the requirement of the forces is the main designing parameter. In contrast to the conventional civil engineering design procedures, where the shape of a structure is predefined and the internal forces are calculated, the forces are predefined here and the shape is searched for. This implies that the structural analysis must be preceded by the form finding analysis to obtain the initial equilibrium position of the structure. The algorithms for this process as well as the proposals of two special stabilization techniques are presented. The numerical examples demonstrate solving of the individual physical or implementation issues.

Structural Analysis

The structural analysis, starting from this initial equilibrium position, is characterized by strong nonlinearities in both the geometrical and the material response. The material lacks the bending stiffness as well as the compressive strength since the stability loss occurs due to the local buckling immediately, even at low compression stress, and exhibit itself as wrinkling of the membrane. The proposed algorithm for dealing with this phenomenon as well as the examples verifying this method are presented.

Cutting Pattern Generation

The other characteristic designing step is the generation of cutting patterns, which is crucial in the manufacturing process. The double-curved shapes of the membrane structures need to be decomposed into pieces, for which the planar approximations are calculated in order to obtain the patterns that can be cut out, assembled and joined together in the subsequent assembly process. This chapter presents the proposed algorithm sequence, further contributed by numerical examples.

Use in Practice

This chapter presents an interesting customer example calculated by using the described and further implemented algorithms.

1.2 OBJECTIVES OF THESIS

Here, the thesis objectives are listed, covering the research work performed.

Form Finding

The objective of this part of the thesis is the description of the general form finding algorithm suitable for the implementation. Furthermore, the aim is also the proposal of an advanced stabilization technique for dealing with conical membranes, which needs special treatment of prestress in the regions of high or low points. In addition to the scope of this thesis, the stabilization technique dealing with the optimization of beams and shell shapes is also proposed and introduced.

Structural Analysis

The aim of this part of the thesis is to deal with the wrinkling phenomenon. Thus, the proposal of the suitable algorithm usable for elastic and inelastic materials is required here. The proposed method should be verified by suitable examples.

Cutting Pattern Generation

The objective of this part of the thesis is the investigation of the existing algorithms for the cutting pattern generation and the consequent proposal of a suitable procedure for the implementation. Thus, the combined procedure composed of two different algorithms is proposed as an optimum solution technique.

The chapters focused on the mentioned objectives are further complemented with the numerical examples calculated by using the FEA solver by the *FEM consulting* company [IV], incorporated into the RFEM software by the *Dlubal Software* company [III]. Thus, the dissertation presents the theoretical research as well as the proposals of the suitable or new algorithms, which were used for the development of the tools for designing and analysing tensile structures in the RFEM software. However, the codes are not a subject of the thesis, but they are a property of these private companies.

2 FORM FINDING

It was already mentioned in the introduction of this thesis, that membrane structures belong to the group of structures, whose shapes cannot be chosen freely as the shape is inherently connected to the equilibrium of forces within the given boundary conditions. For a civil engineer or an architect designing these structures, the equilibrium of the internal and external forces within the frame of the defined boundaries are the shaping parameters as well as the degree of freedom. The typical

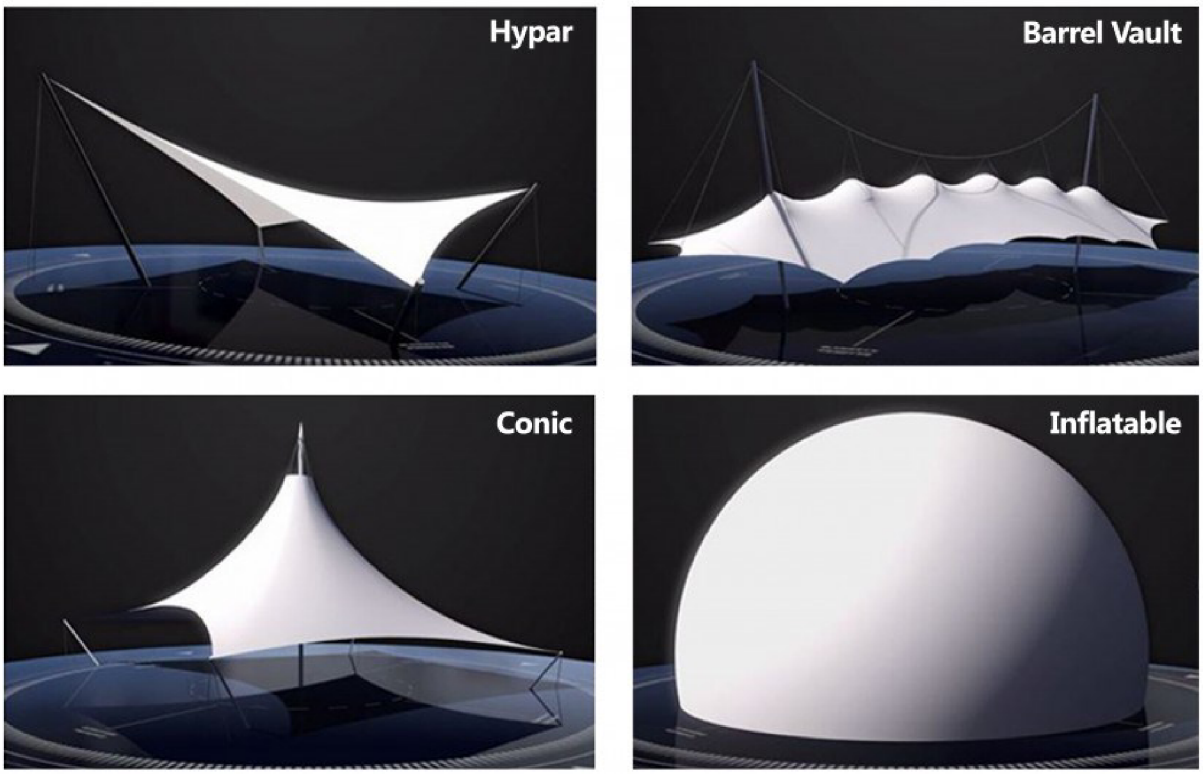

Fig. 3 Categorization of Membrane Structure Shapes [V]

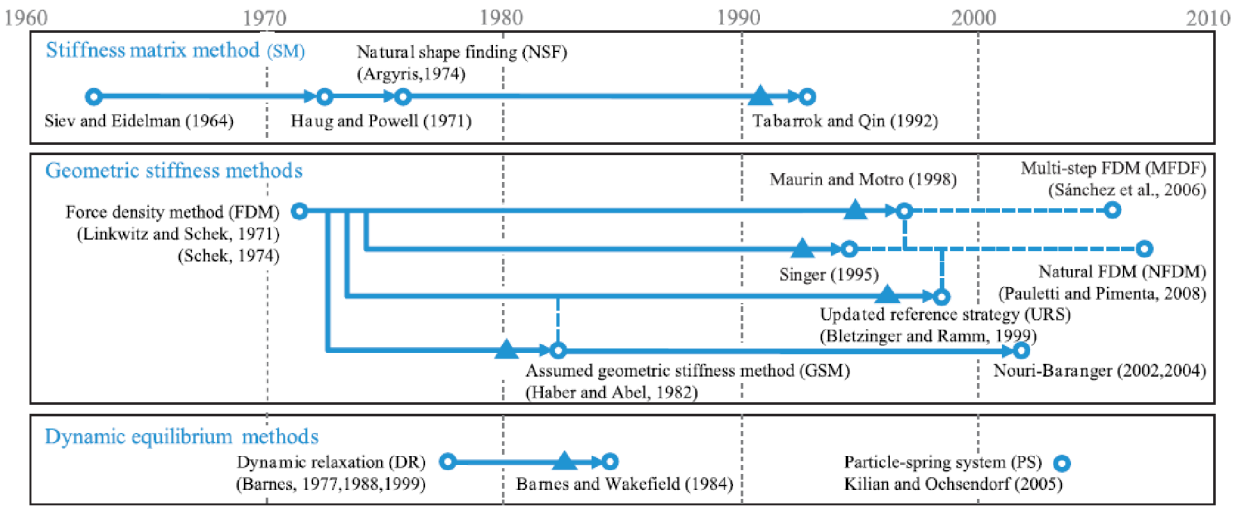

Fig. 4 Categorization of Form Finding Methods aAccording to D. Veenendaal and P. Block [8].

double curvature is the characteristic aesthetic appearance as well as the necessity of the structures to be satisfied, in connection with the internal forces, to reach the required load bearing capacity. Some of the basic shapes are displayed in the figure above (Fig. 3).

According to the paper written by the authors D. Veenendaal and P. Block [8], the following categorization of the form finding methods can be assumed (Fig. 4).

2.1 SEARCHING FOR EQUILIBRIUM PRESTRESS

The name form finding is suggesting the searching process for a shape when the equilibrium prestress is explicitly known and thus given. However, this is generally not a true. The constant orthotropic prestress cannot exist in the surface with double curvature, so the general anisotropic stress field has to be reached if the isotropic prestress does not satisfy the engineering or architectural requirements for the given tensile structure. Such a user entry is not realistic and therefore, the constant values in the orthogonal directions, called warp and weft, are the usual software entries. The resulting prestress should approximate the given values. However, when the given values are strongly enforced, all the methods would collapse.

Thus, the process should be understood as the **initial equilibrium problem** as besides the shape, the calculation also comprises finding of the equilibrium of forces itself. For this issue, many stabilization techniques were proposed, such as: *Specifying Number of Form Finding Steps*, *Elastic Control*, *Element Size Control*, *Projection Method*, etc.

2.2 PROJECTION METHOD

As this method was proposed within the scope of the presented thesis, it will be described shortly below. The basic idea of this method is to prescribe the equilibrium in the projection plane, where it is possible to do it directly by analytical formulas and afterwards to transform this prestress into the spatial configuration of the structure.

The process could be described by using an artificial deformation gradient ${}^{t}_{p}\mathbf{F}$. This tensor describes a virtual deformation, which would be performed to move the fictitious FE, obtained by the projection of the real FE into the projection plane, back to the real FE position in the particular iteration. Based on this tensor, the Cauchy stress ${}^{t}\boldsymbol{\sigma}$ in the actual FE configuration can be obtained

$$ {}^{t}\boldsymbol{\sigma} = \frac{{}^{t}\rho}{{}_{p}\rho}\, {}^{t}_{p}\mathbf{F}\, {}^{t}_{p}\mathbf{S}\, {}^{t}_{p}\mathbf{F}^{T} = \frac{1}{\det\left({}^{t}_{p}\mathbf{F}\right)}\, {}^{t}_{p}\mathbf{F}\, {}^{t}_{p}\mathbf{S}\, {}^{t}_{p}\mathbf{F}^{T} \tag{2.1} $$

Using this implicit manner of the spatial equilibrium prestress definition (Fig. 5), the input values for the general materially independent formula are defined

$$\int_{{}^{t}V} {}^{t}\boldsymbol{\sigma}\, \delta_{t}\boldsymbol{\eta}\, {}^{t}dV = {}^{t+\Delta t}\boldsymbol{\mathcal{R}} - \int_{{}^{t}V} {}^{t}\boldsymbol{\sigma}\, \delta_{t}\boldsymbol{\varepsilon}\, {}^{t}dV \tag{2.2}$$

This leads to the unique solution, which is independent of the initial shape configuration. This is a great advantage of this *projection method* stabilization technique, because such a behaviour is usually considered as valid for the isotropic prestress only.

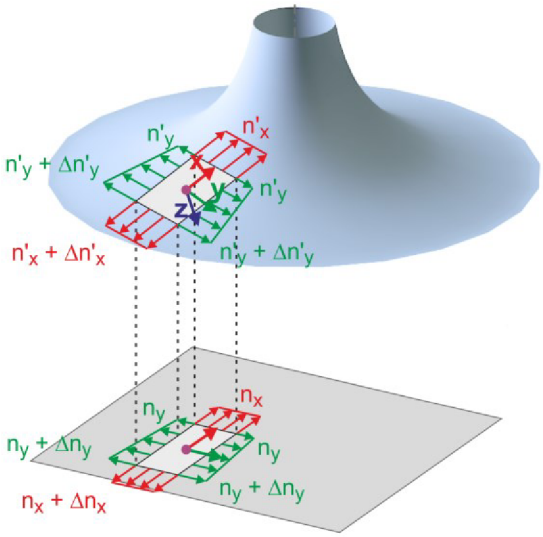

Fig. 5 Prestress Defined in Projection Plane and Prestress in Membrane Structure

2.3 PUSHING METHOD FOR COMPRESSION REQUIREMENTS IN FORM FINDING PROCESS

During the research and the development works of the form finding process of membrane structures, including shaping the cables and gas chambers, the shape optimization of the conventional structures was also additionally investigated. Since the load bearing capacity is increased for both the arches and the shells, if the in-plane resistance is preferred form of the bending resistance.

A physically new phenomenon has to be dealt with here, as in the contrast to the tensile definitions, which could be considered as a stable equilibrium state finding, the unstable equilibrium searching is the case when the compression requirements are prescribed. Since the tensile forces try to reach the stable equilibrium from the arbitrary non-equilibrium position, as illustrated in the left part of the figure below, the compression forces try to diverge far away from the given non-equilibrium position, as illustrated by the right part of the figure below (Fig. 6).

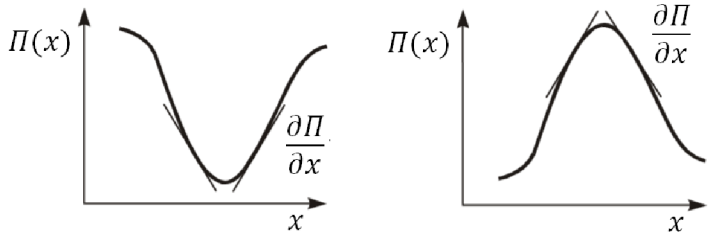

Fig. 6 Stable and Unstable Equilibrium Position

Therefore, the proposed stabilization, called here as a *pushing method,* tries to push up the structure to the maximum energy position, which is represented by the top position in the right part of the figure above (Fig. 6). The process consists physically of two artificial modifications during assembling the equilibrium equations. The first modification inserts an artificial geometric stiffness into the elements with the compression requirement. The second, more sensitive and important modification, deals with inverting the unbalanced forces in the appropriate FE nodes, where the unstable equilibrium is expected [15].

$$\Delta\mathbf{R} = {}^{t+\Delta t}_{t}\mathbf{R} - {}^{t}\mathbf{F} \tag{2.3}$$

$$\Delta\mathbf{R}_i = \begin{cases} \Delta\mathbf{R}_i = -\Delta\mathbf{R}_i & i \in U \\ \Delta\mathbf{R}_i & i \in S \end{cases} \tag{2.4}$$

where i is the number of particular FE node, U and S are the groups of nodes, where the unstable and stable equilibrium is expected.

It is crucial to do this inversion as post-processing after the standard assembling process of the unbalanced forces is ready, since it is necessary to preserve the magnitude, but change the direction. Finally, the decision of the group membership for the individual nodes is quite a sensitive task. In this proposal, it is suggested that this is performed according to the hierarchy algorithm.

2.4 IMPLEMENTED FORM FINDING METHODS

Two form finding methods were implemented, the first one used as a *default* procedure, considering all the structural parts, and the second one used as a *preliminary* form finding, considering only the structural parts with the definition of the required forces.

2.4.1 Preliminary Form Finding

To implement the *preliminary form finding,* the *GSM* group was chosen, specifically the *AGSM* with *ISM*.

For stabilizing the non-equilibrium prestress definition, the *preliminary form finding* uses three possible stabilizations: first, the simple influencing of step numbers by a user, further the calculation interruption based on the deformation monitoring algorithm, and finally a possible usage of the projection method.

2.4.2 Default Form Finding

The *default form finding* can be classified as a *hybrid method*, which balances between the *GSM* and *SM* groups.

For stabilizing the non-equilibrium prestress definition, the *default form finding* uses the *controlling* way of the *elastic control*, the deformation monitoring and the equilibrium finding when deformations normal to the plane start to be minor in comparison with the tangential deformations and the possible usage of the projection method can be included as well. The setting of a number of the form finding steps can also be influenced.

2.5 EXAMPLES

In the following, there are some examples of the form finding analyses presented in context with the particular phenomena. More complex structures are also shown later to present the abilities of the implemented algorithms.

2.5.1 Independence of Equilibrium Shape on Initial Model Position

The resulting shape (Fig. 8) is dependent exclusively on the predefined equilibrium of forces and the given boundary conditions. This fact is presented in the next example of a hypar shaped membrane (Fig. 3), where two different initial configurations were chosen (Fig. 7). The isotropy prestress of the membrane is $n_x = n_y = 1.00\,kN/m$ and the tension in the cables is $N = 10.00\,kN$.

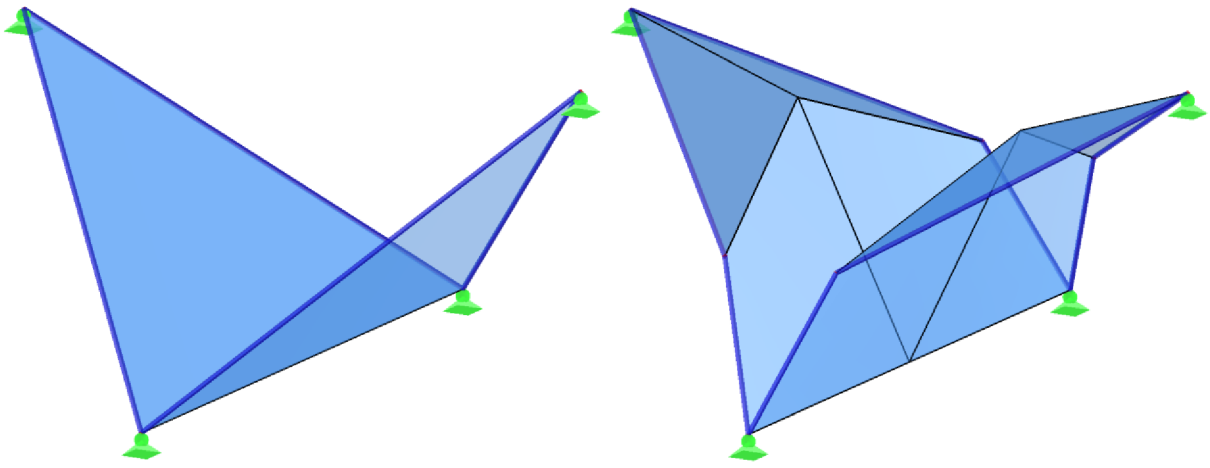

Fig. 7 Initial Geometry of Two Hypar Membranes

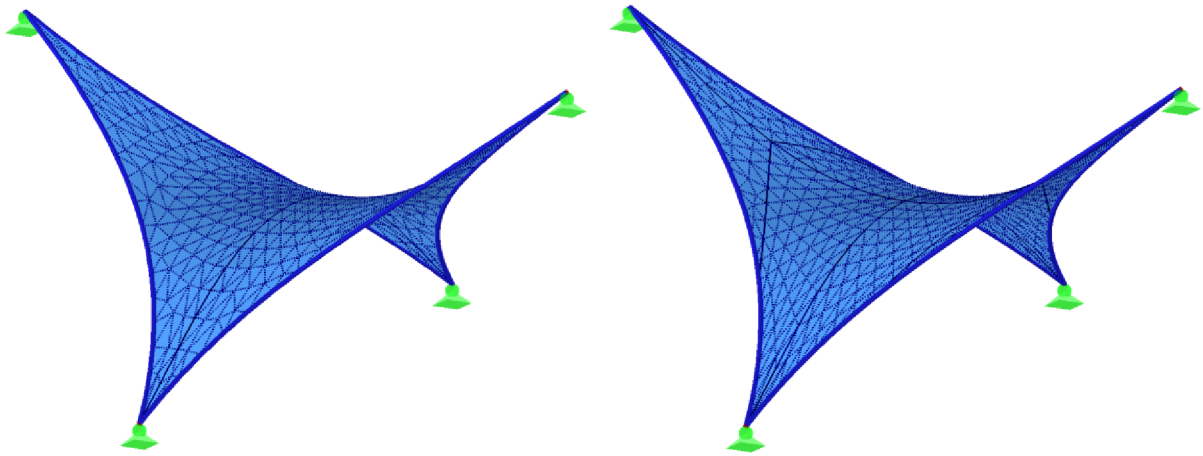

Fig. 8 Final Geometry and FE Mesh of Two Hypar Membranes

2.5.2 Projection Method

The following example shows the umbrella membrane with the square base made of cables (Fig. 9). Such conical shapes are typical by necessity of the stress concentration in the regions of the top or bottom rings. Here, the given prestress values $n_x = n_y = 1.00\ kN/m$ will be far away from the resulting prestress of the membrane. To be complete, the prestress $N = 5.00\ kN$ for the boundary cables is required.

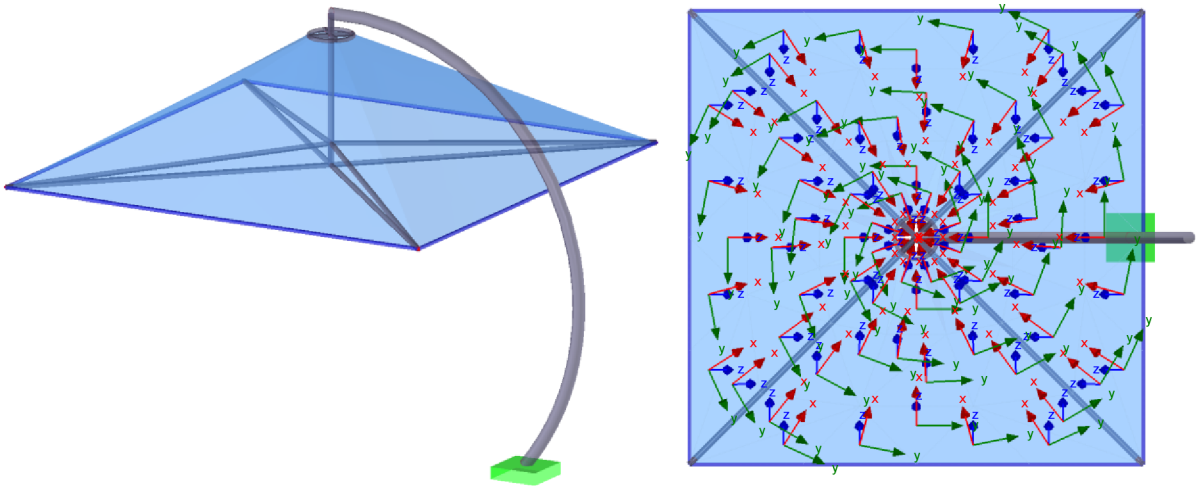

Fig. 9 Initial Model Position of Membrane Umbrella (Light Blue: Membrane, Blue: Cables, Gray: Beams) and Axis Orientation: x (Radial), y (Tangential)

Two stabilization procedures are compared here, specifically the Specifying Number of Form Finding Steps and the Projection Method. In the figures below, the axial prestress n_x generated by these procedures is observable for the overall structure. Further, the prestress in the bottom corner is compared using a vector displaying.

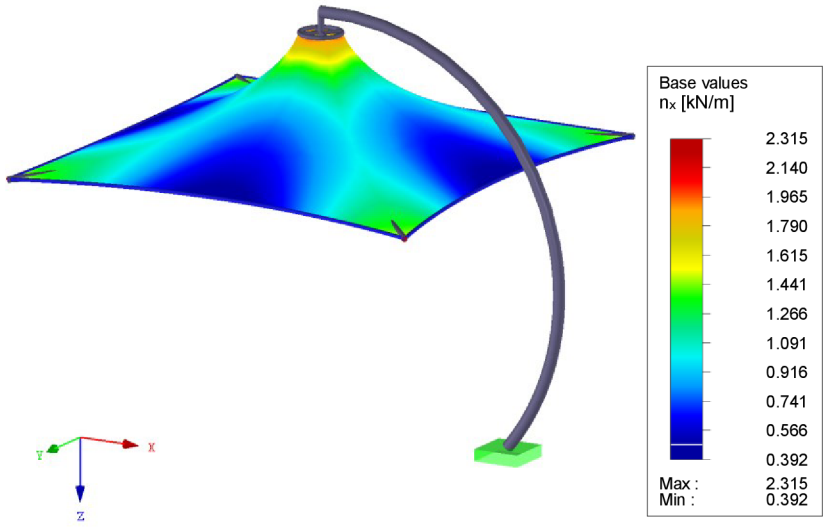

Fig. 10 Normal Forces in x Direction; Stabilization: Specifying Number of Form Finding Steps

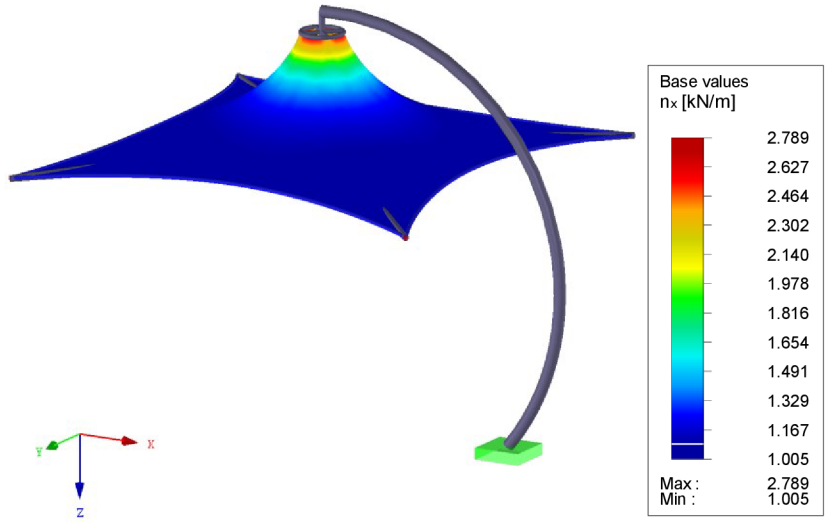

Fig. 11 Normal Forces in x Direction; Stabilization: Projection Method

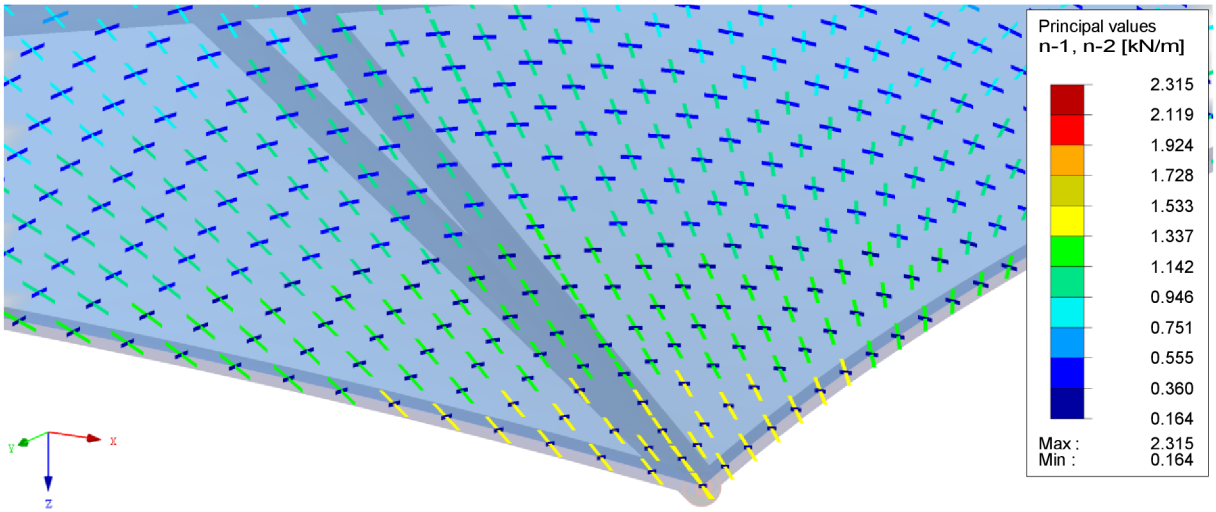

Fig. 12 Principal Forces Vectors in Corner of Left Membrane; Stabilization: Specifying Number of Form Finding Steps

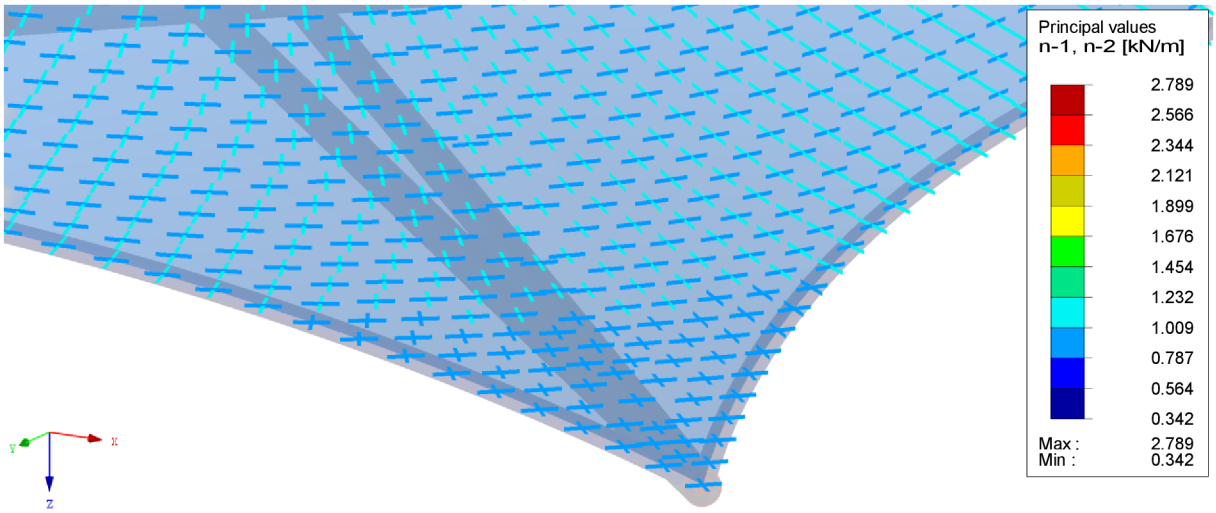

Fig. 13 Principal Forces Vectors in Corner of Left Membrane ; Stabilization: Projection Method

While comparing the results, the non-smooth prestress is reached by the first stabilization technique *Specifying Number of Form Finding Steps*, since this method works as a safety brake and does not lead to a unique prestress. As well as the other methods, such as Elastic Control, Element Size Control, etc., this method is distinguished by the dependence between the initial and the resulting shape. Thus, the prestress cannot be driven directly.

In contrast to these properties, the *Projection Method* has the unique indepencency of the resulting prestress of the initial shape approximation. Thus, the prestress can be driven much more directly. The prestress, generated on the basis of the isotropic input values, has much smoother character as can be seen while observing the figures (Fig. 10, Fig. 11, Fig. 12, Fig. 13).

2.5.3 Possibility of Multiple Equilibrium Solutions for Some Form Finding Analyses

The following example demonstrates the combination of the form finding process for membranes and cables with the procedure of the shape optimization for two arches. For comparison purposes, three cases are considered. First, the arches are not shaped, but given, then two cases of the arches shaping are assumed. The required resulting length of the second and the third example is defined to be the same as the length in the first example.

As the shapes of the arches in the second and the third example are optimized to restrict in the normal direction, the shear forces and bending moments are virtually zero (Fig. 15). in this case. Moreover, the very interesting phenomenon occurs here, more equilibrium solutions could exist when mixed (positive and negative) requirements are assumed (Fig. 14).

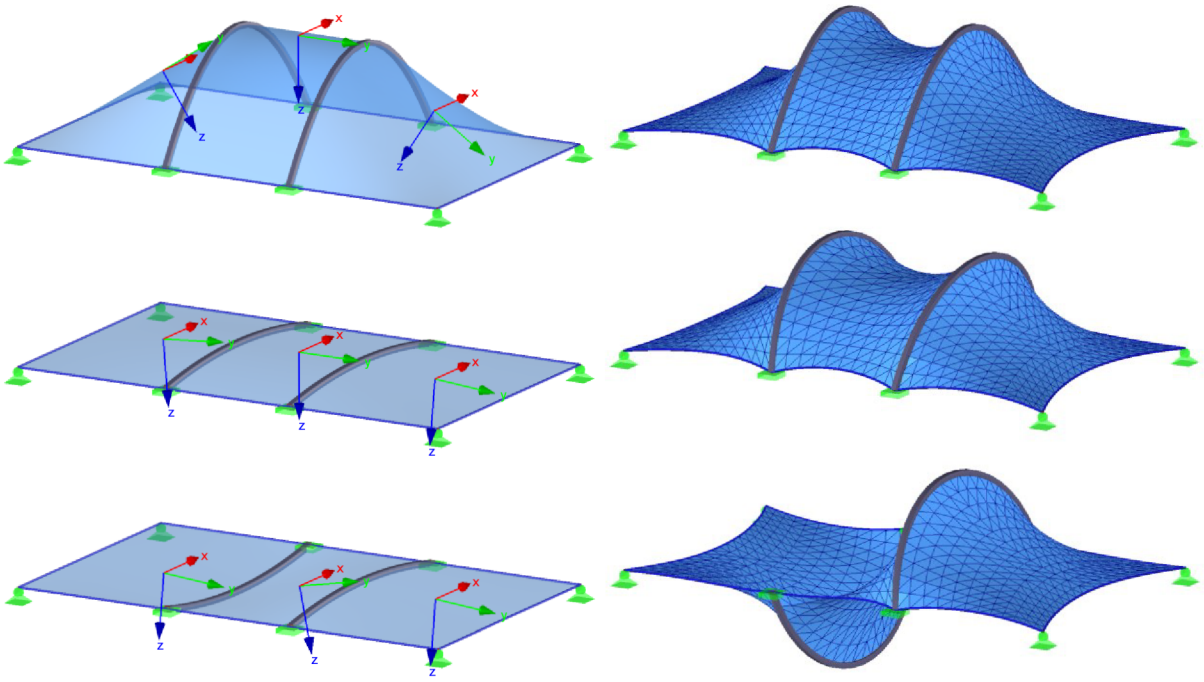

Fig. 14 Initial Model Positions with x and y Axis Orientation (left), Final Geometry and FE Mesh Discretization (right)

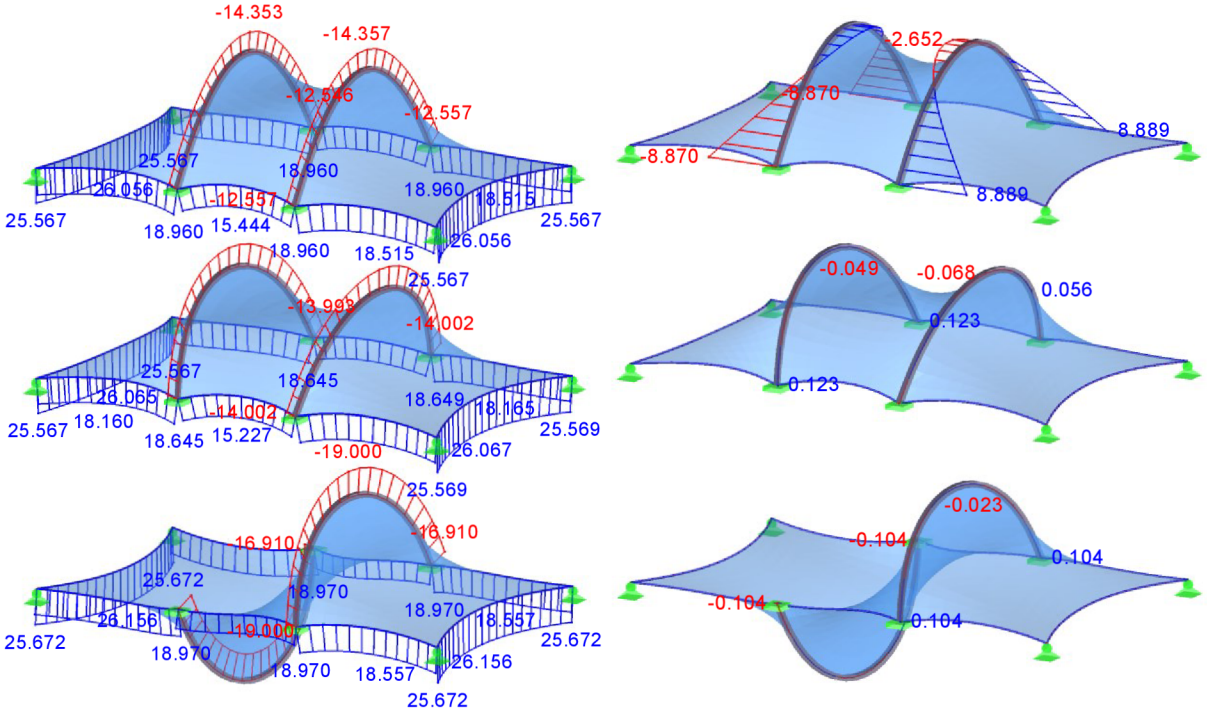

Fig. 15 Normal Forces N $[kN]$ (left), Bending Moments M_z $[kN/m]$ (right)

2.5.4 Examples of Complex Structures

Now, there are few other structures of more complex compositions shown for illustrative purposes (Fig. 16 – Fig. 19). Therefore, the initial and equilibrium shapes are shown without a detailed description.

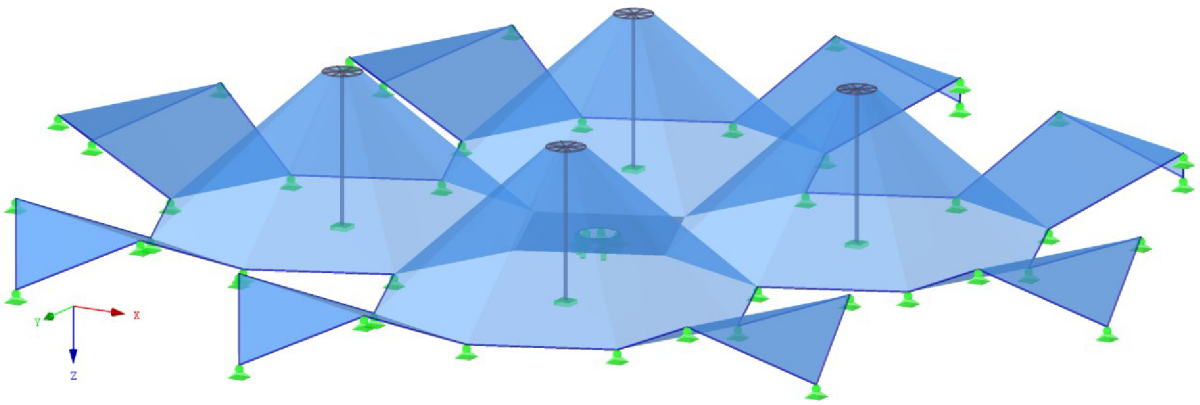

Fig. 16 Composition of Conical and Hypar Membranes – Initial Position [11]

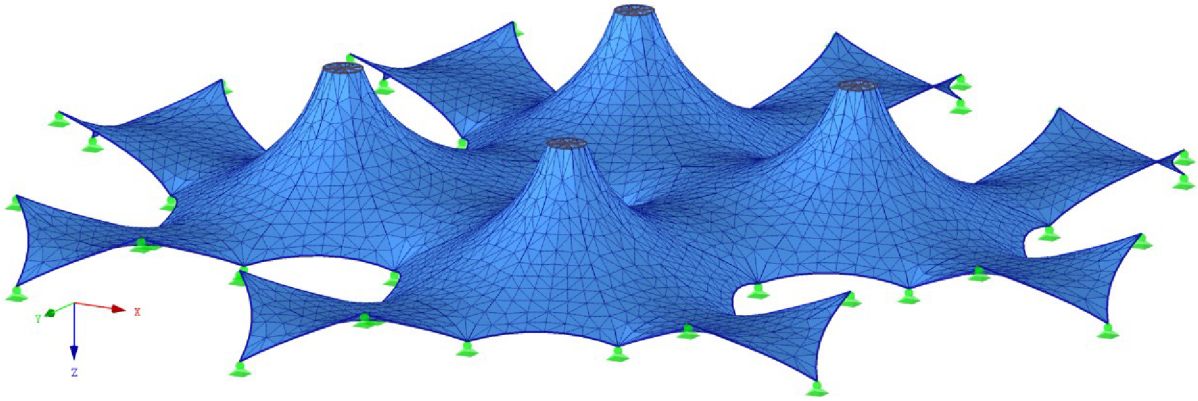

Fig. 17 Composition of Conical and Hypar Membranes – Equilibrium Position [11]

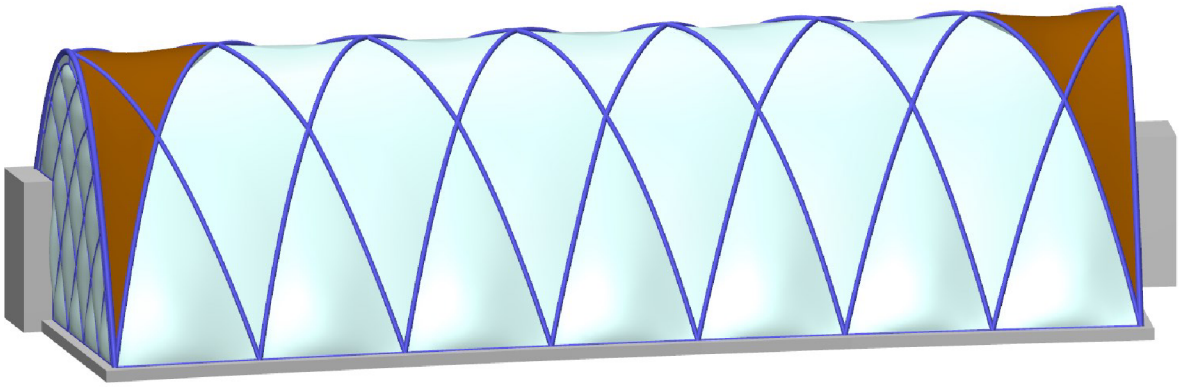

Fig. 18 Greenhouse Made of Pressurized ETFE Cushions – Initial Model [11]

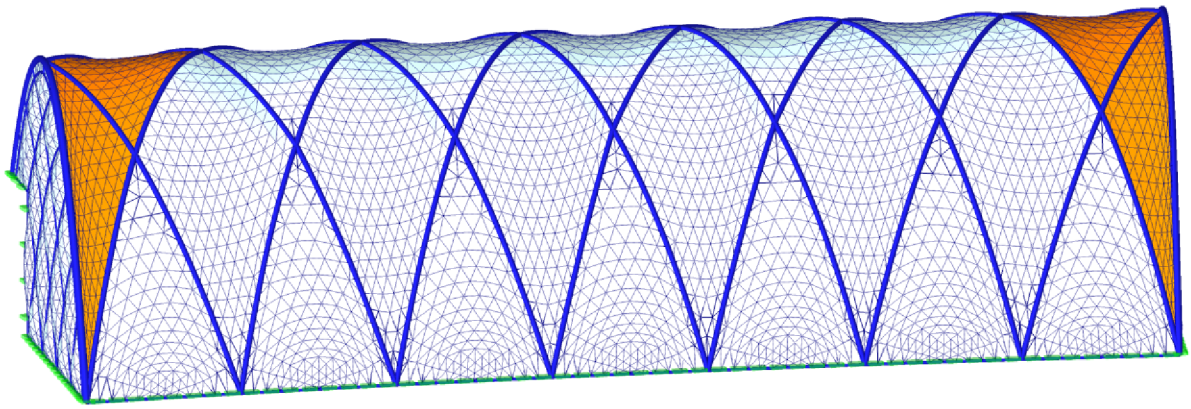

Fig. 19 Greenhouse Made of Pressurized ETFE Cushions – Equilibrium Position [11]

3 STRUCTURAL ANALYSIS

Membrane structures are really special in analysis requirements, which is the consequence of their virtually zero bending stiffness. That implies the singularity when the material stiffness matrix is only taken into account. Thus, the geometric stiffness matrix needs to be regular, which implies tension in the whole membrane. Therefore, if compression occurs, a special treatment has to be performed in the implemented codes. This is done by applying an artificial minimal tension in the numerical analysis.

Moreover, the material nonlinearity of membrane structures is quite a unique issue. If a membrane loses its pretension, the compression is released by the surface wrinkling and the standard membrane theory does not describe such a state. This is one of the most important and difficult tasks of the structural analysis of such a type of structures.

Within this chapter, the proposed methods called ***Wrinkling Separation*** and ***Elastic Prediction Modification*** are presented. The formulated methods are further analysed on verification examples.

3.1 WRINKLING OF MEMBRANE SURFACES

The *Tension Field Theory (TF)* assumes that a membrane has zero flexural stiffness. While the membrane is stretched, the classic membrane theory for the evaluation of the stress state is valid. However, when the compression is about to appear, in the consequence of the zero flexural stiffness assumption, the compression is immediately released by the buckling effect, thus by the development of little waves aligned with the tensile direction (Fig. 20).

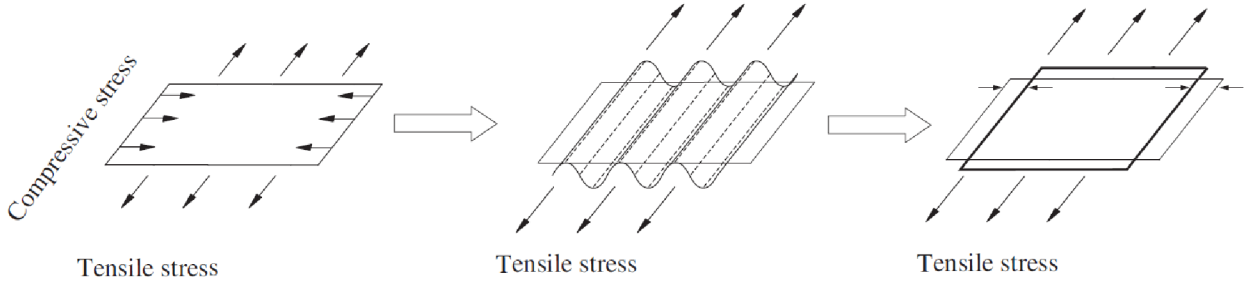

Fig. 20 Applied Stress (left), Real Physical Deformation (Wrinkling) of Membrane (middle), In-Plane Deformation/Strain (right). [12]

3.2 WRINKLING CRITERIA

In order to determine the actual state of the membrane, the wrinkling criteria were developed to distinguish whether the membrane is in a taut, wrinkled or slack state (Tab. 1, Fig. 21).

Tab. 1 Wrinkling Criteria to Distinguish Membrane Status

Membrane state	Principal stress criteiron	Principal strain criterion	Mixed criterion
Taut	$S_{min} > 0$	$E_{min} > 0$	$S_{min} > 0$
Wrinkled	$S_{min} \leq 0$ and $S_{max} > 0$	$E_{min} \leq 0$ and $E_{max} > 0$	$S_{min} \leq 0$ and $E_{max} > 0$
Slack	$S_{min} \leq 0$ and $S_{max} \leq 0$	$E_{min} \leq 0$ and $E_{max} \leq 0$	$E_{max} \leq 0$

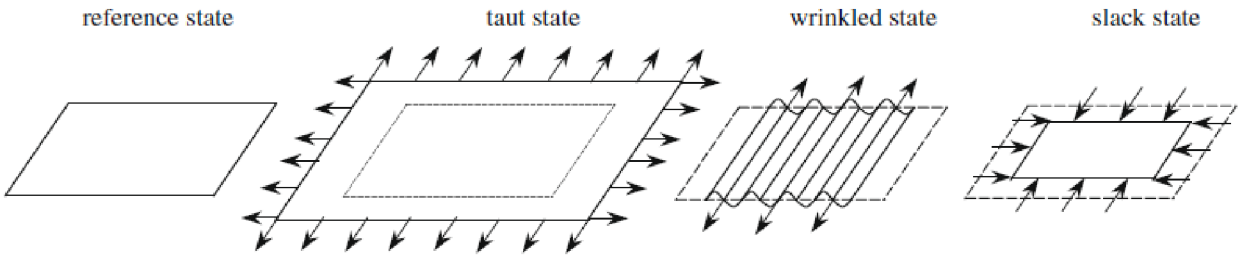

Fig. 21 State of Membrane: Taut, Wrinkled and Slack [10]

The principal stress and principal strain criterion can be misleading. Therefore, the mixed criterion is considered and widely used as a suitable choice.

3.3 WRINKLING SEPARATION AND ELASTIC PREDICTION MODIFICATION

The proposal of a new technique dealing with the wrinkling phenomenon described above was made. The actual strain is decomposed into the real in-plane and wrinkling components and the fictitious stress is decomposed into the real and non-physical parts, released by the local buckling process.

3.3.1 Wrinkling Separation Procedure for Anisotropic Linear Elastic Material Models

The whole process is described on the level of each FE integration point. The total strain is decomposed and the constitutive matrix is derived. First, the elastic stress estimation in the planar Cartesian coordinate system is performed

$$\boldsymbol{\sigma} = \mathbf{C}\,\boldsymbol{\varepsilon} \tag{3.1}$$

Further, the stress is transformed into the main directions

$$\boldsymbol{\sigma} \rightarrow \bar{\boldsymbol{\sigma}} = [\ \bar{\sigma}_1 \quad \bar{\sigma}_2 \quad 0\ ]^{\mathrm{T}} \tag{3.2}$$

If the membrane is classified to be in wrinkled state, the **Wrinkling Separation** procedure uses the above-defined assumption that the negative stress $\bar{\sigma}_2$ is released by the local buckling effect and thus the real elastic stress $\bar{\sigma}_2^e = 0$. As the value of $\bar{\sigma}_1$ is influenced by the coefficient of the transverse contraction even for the wrinkling part of the strain, its value is not correct and thus the elastic stress $\bar{\sigma}_1^e$ is set as unknown $\bar{\sigma}_1^e = ?$. Furthermore, $\bar{\varepsilon}_{11}^e = \bar{\varepsilon}_{11}$, $\bar{\varepsilon}_{22}^e \neq 0$ and $\bar{\varepsilon}_{12}^e \neq 0$ generally.

$$\begin{bmatrix} \bar{\sigma}_1^e = ? \\ 0 \\ 0 \end{bmatrix} = \begin{bmatrix} \bar{C}_{1111} & \bar{C}_{1122} & \bar{C}_{1112} \\ \bar{C}_{2211} & \bar{C}_{2222} & \bar{C}_{2212} \\ \bar{C}_{1211} & \bar{C}_{1222} & \bar{C}_{1212} \end{bmatrix} \begin{bmatrix} \bar{\varepsilon}_{11}^e = \bar{\varepsilon}_{11} \\ \bar{\varepsilon}_{22}^e = ? \\ \bar{\varepsilon}_{12}^e = ? \end{bmatrix} \tag{3.3}$$

Using this procedure, the elastic components of the in-plane deformation are separated out. If the membrane status is taut, the original constitutive matrix is valid $\mathbf{C}_\mathrm{t} = \mathbf{C}$, and if the membrane status is slack, the constitutive matrix $\mathbf{C}_\mathrm{s}$ becomes a zero matrix. If the membrane is in the wrinkled status, the constitutive matrix $\mathbf{C}_\mathrm{w}$ can be calculated numerically

$$\mathbf{C}_\mathrm{w} = \begin{bmatrix} \frac{\partial \sigma_{11}}{\partial \varepsilon_{11}} & \frac{\partial \sigma_{11}}{\partial \varepsilon_{22}} & \frac{\partial \sigma_{11}}{\partial \varepsilon_{12}} \\ \frac{\partial \sigma_{22}}{\partial \varepsilon_{11}} & \frac{\partial \sigma_{22}}{\partial \varepsilon_{22}} & \frac{\partial \sigma_{22}}{\partial \varepsilon_{12}} \\ \frac{\partial \sigma_{12}}{\partial \varepsilon_{11}} & \frac{\partial \sigma_{12}}{\partial \varepsilon_{22}} & \frac{\partial \sigma_{12}}{\partial \varepsilon_{12}} \end{bmatrix} \tag{3.4}$$

Moreover, it can be proven that for the isotropic material, the following analytical constitutive relation holds

$$\mathbf{C}_\mathrm{w} = \begin{bmatrix} E & 0 & 0 \\ 0 & 0 & 0 \\ 0 & 0 & k\,G \end{bmatrix} = \begin{bmatrix} E & 0 & 0 \\ 0 & 0 & 0 \\ 0 & 0 & k\,\dfrac{E}{2(1+\nu)} \end{bmatrix} \tag{3.5}$$

where k is the coefficient of the shear softening, which is dependent on the degree of wrinkling, thus on the relation of the elastic and the total strains

$$k = \frac{\varepsilon_{12}^e}{\varepsilon_{12}} = \frac{\varepsilon_{11}^e - \varepsilon_{22}^e}{\varepsilon_{11} - \varepsilon_{22}} \tag{3.6}$$

For the sake of the FEA numerical stability, the real tangential stiffness $\mathbf{C}_\mathrm{s}$ or $\mathbf{C}_\mathrm{w}$ cannot be used directly as it leads to the oscillations of forces and the deformations during the calculation, and the analysis often does not even converge at all. Thus, the artificial stiffness modification applies in order to avoid such behaviour.

3.3.2 Elastic Prediction Modification for Nonlinear Elastic and Plastic Material Models

The process is further extended for the application in the case of the nonlinear elastic or plastic material models. The proposed calculation procedure is represented by the attached figures (Fig. 22, Fig. 23), and can be described by the consequent flowchart. For the sake of different elastic prediction distinctions, the left index is added. Moreover, to be consistent in the notation of the formulas, the bar above the stress vectors and components is used, since the main directions are assumed in the following formulas.

I. The calculation of the standard elastic prediction ${}^{\mathrm{I}}\bar{\boldsymbol{\sigma}} = [\ {}^{I}\bar{\sigma}_1 \quad {}^{I}\bar{\sigma}_2 \quad 0\ ]^{\mathrm{T}}$

II. The modification of the elastic prediction by the wrinkling separation procedure ${}^{\mathrm{II}}\bar{\boldsymbol{\sigma}} = [\ {}^{II}\bar{\sigma}_1 \quad 0 \quad 0\ ]^{\mathrm{T}}$

III. Performing the return algorithm to the yielding surface, representing the chosen criterion with the consideration of the additional elastic prediction modification ${}^{\mathrm{III}}\bar{\boldsymbol{\sigma}} = [\ {}^{III}\bar{\sigma}_1 \quad {}^{III}\bar{\sigma}_2 \quad 0\ ]^{\mathrm{T}}$ and thus converging to the final stress state $\bar{\boldsymbol{\sigma}}^{\mathrm{e}} = [\ \bar{\sigma}_1^{e} \quad \bar{\sigma}_2^{e} \quad 0\ ]^{\mathrm{T}}$.

Since the first two steps are the same as in the previous subchapter (3.3.1), the last step needs to be described in more detail.

Let's assume the return process from the elastic prediction modified by the wrinkling separation algorithm ${}^{\mathrm{II}}\bar{\boldsymbol{\sigma}} = [\ {}^{II}\bar{\sigma}_1 \quad 0 \quad 0\ ]^{\mathrm{T}}$. The stress change caused by the yielding process can be described as

$$\boldsymbol{\Delta\bar{\sigma}} = [\Delta\bar{\sigma}_1 \quad \Delta\bar{\sigma}_2 \quad 0] \tag{3.7}$$

When observing this process in two following figures (Fig. 22, Fig. 23), the origination of the tensile force $\Delta\sigma_2$ in the wrinkled direction is obvious. However, the fictitious compression component $\bar{\sigma}_2^{\mathrm{W}}$ of the eliminated fictitious stress state $\bar{\boldsymbol{\sigma}}^{w} = [\bar{\sigma}_1^{w} \quad \bar{\sigma}_2^{w} \quad 0]$ was separated out by the wrinkling separation procedure (note: $\bar{\sigma}_2^{w} = {}^{I}\bar{\sigma}_2$). Thus, the tension increment $\Delta\bar{\sigma}_2$ cannot be the final stress state. Thus, the elastic prediction ${}^{\mathrm{II}}\bar{\boldsymbol{\sigma}}$ is further modified to ${}^{\mathrm{III}}\bar{\boldsymbol{\sigma}}$. Two essential cases can be described by the following formulas:

$$\bar{\sigma}_2^{w} + \Delta\bar{\sigma}_2 \leq 0 \longrightarrow {}^{\mathrm{III}}\bar{\boldsymbol{\sigma}} = [\ {}^{III}\bar{\sigma}_1 \quad {}^{III}\bar{\sigma}_2 \quad 0\ ]^{\mathrm{T}} = [\ {}^{II}\bar{\sigma}_1 \quad -\Delta\bar{\sigma}_2 \quad 0\ ]^{\mathrm{T}} \tag{3.8}$$

$$\bar{\sigma}_2^{w} + \Delta\bar{\sigma}_2 > 0 \longrightarrow {}^{\mathrm{III}}\bar{\boldsymbol{\sigma}} = [\ {}^{III}\bar{\sigma}_1 \quad {}^{III}\bar{\sigma}_2 \quad 0\ ]^{\mathrm{T}} = [\ {}^{II}\bar{\sigma}_1 \quad {}^{I}\bar{\sigma}_2 \quad 0\ ]^{\mathrm{T}} \tag{3.9}$$

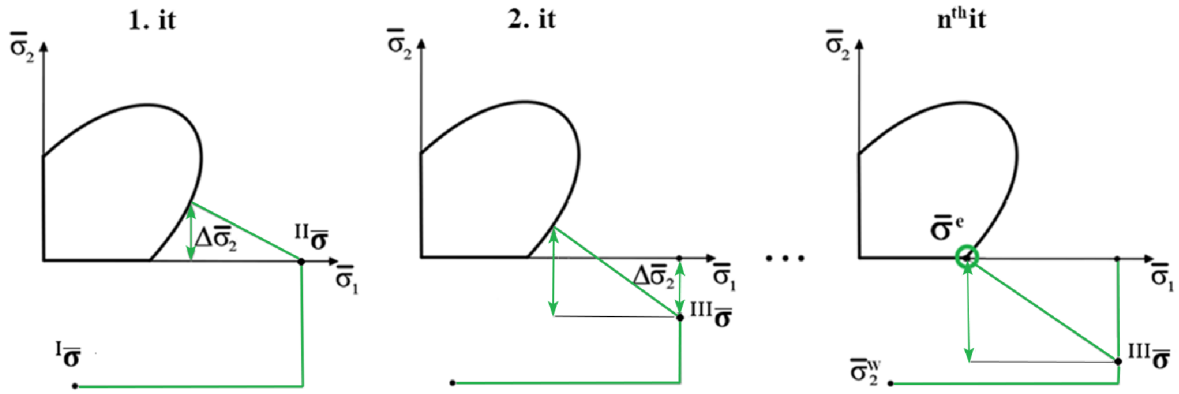

Fig. 22 Standard Elastic Prediction ${}^{I}\bar{\boldsymbol{\sigma}}$ and Elastic Prediction after Wrinkling Separation ${}^{II}\bar{\boldsymbol{\sigma}}$ (left), Iterative Modification of Elastic Prediction ${}^{III}\bar{\boldsymbol{\sigma}}$ (middle and right), Final Elastic Prediction ${}^{III}\bar{\boldsymbol{\sigma}}$ and Resulting Stress State $\bar{\boldsymbol{\sigma}}^{e}$ (right). Iteration Counter (Above).

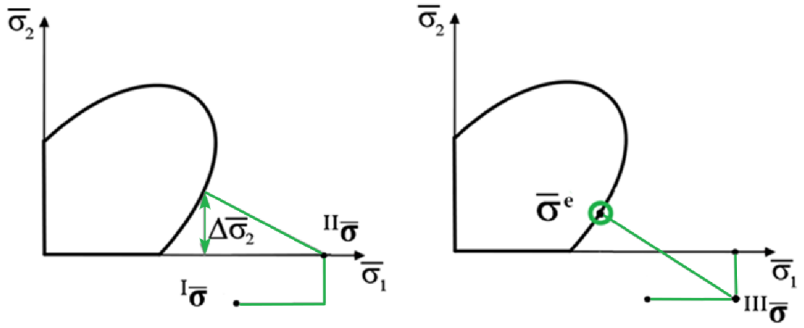

Fig. 23 Standard Elastic Prediction ${}^{I}\bar{\boldsymbol{\sigma}}$ and Elastic Prediction After Wrinkling Separation ${}^{II}\bar{\boldsymbol{\sigma}}$ (left), Modification of Elastic Prediction ${}^{III}\bar{\boldsymbol{\sigma}}$ and Resulting Stress State $\bar{\boldsymbol{\sigma}}^{e}$ (right).

Finally, the real stress state is estimated and the transformation into the planar Cartesian coordinate directions can be performed, holding the well-known equation $\boldsymbol{\sigma} = \mathbf{C}\,(\boldsymbol{\varepsilon} - \boldsymbol{\varepsilon}^{\mathrm{p}} - \boldsymbol{\varepsilon}^{\mathrm{w}})$, which was extended with the strain representing the wrinkling $\boldsymbol{\varepsilon}^{\mathrm{w}}$.

The main advantage of the proposed method of the **wrinkling separation** and the consequent **elastic prediction modification** is in its modularity. As this process originates from the mentioned modification of the elastic prediction, it does not change the definition of the used material yielding criterion itself. The return algorithms and the constitutive matrices can be then used in a standard manner.

3.4 NUMERICAL EXAMPLES

This chapter presents numerical examples. First, the wrinkling separation procedure for the linear elastic material models is verified on an example with the analytical solution available. Further, other examples are presented, also covering the nonlinear material models.

3.4.1 Pure Bending of Rectangular Membrane

As a first example, the well-known and often used pure bending of the stretched rectangular membrane is chosen (Fig. 24). This example has an analytical solution [13] and therefore, it serves as a benchmark when evaluating the wrinkling separation process for elastic materials.

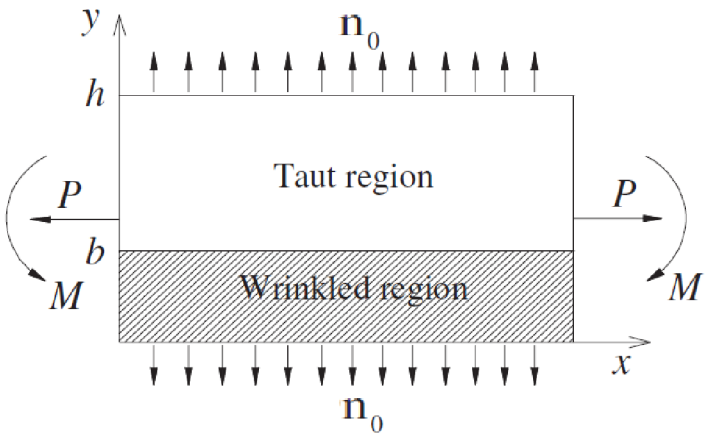

Fig. 24 Pure Bending of Stretched Rectangular Membrane [12]

The comparison of the gradual spreading of the wrinkled region for the analytical and numerical solutions could be observed in the following figure (Fig. 25). These results prove the reliability of the proposed method.

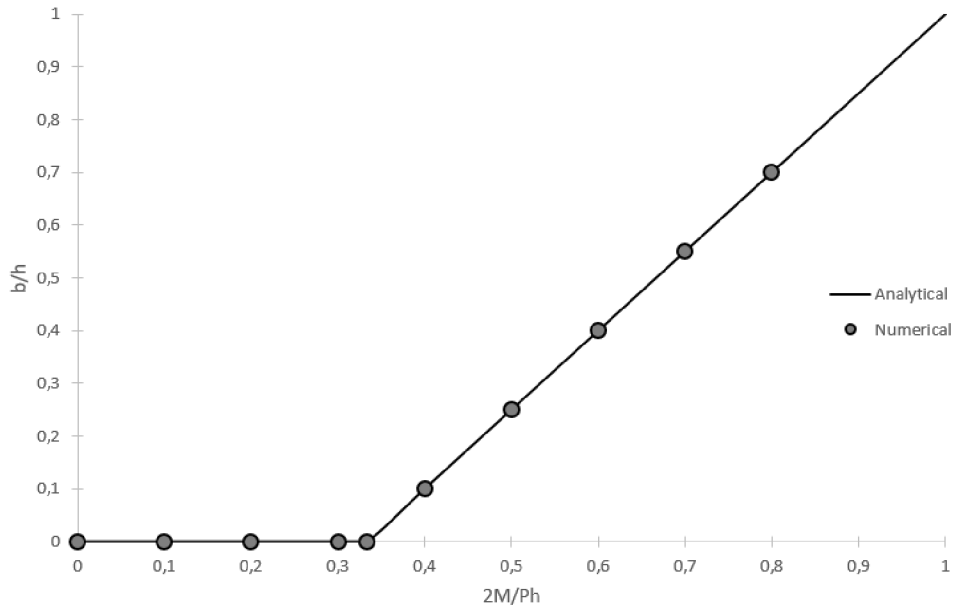

Fig. 25 Spreading of Wrinkled Region Bandwidth b in Dependence on Applied Moment M

3.4.2 Shear Test of Rectangular Membrane for Orthotropic Elastic Material

In the second example, the shear test of the rectangular membrane is performed. As there is no analytical solution defined, another proof of the result reliability is used.

The method is verified by comparing the results performed by two analysis ways, which converges to the same solution gradually. The examples will use the wrinkling separation as well as the extensive refinement of the FE. Thus, the mesh dependence is also presented here in the form of a graph.

$E_x = 2000.0\,kN/m$, $E_y = 1000.0\,kN/m$, $G = 200.0\,kN/m$, $\nu_{xy} = 0.20$, the rectangular length $l = 2.0\,m$, height $h = 1.0\,m$ and thickness $t = 1.0\,mm$, the imposed deformation $\Delta = 100.0\,mm$.

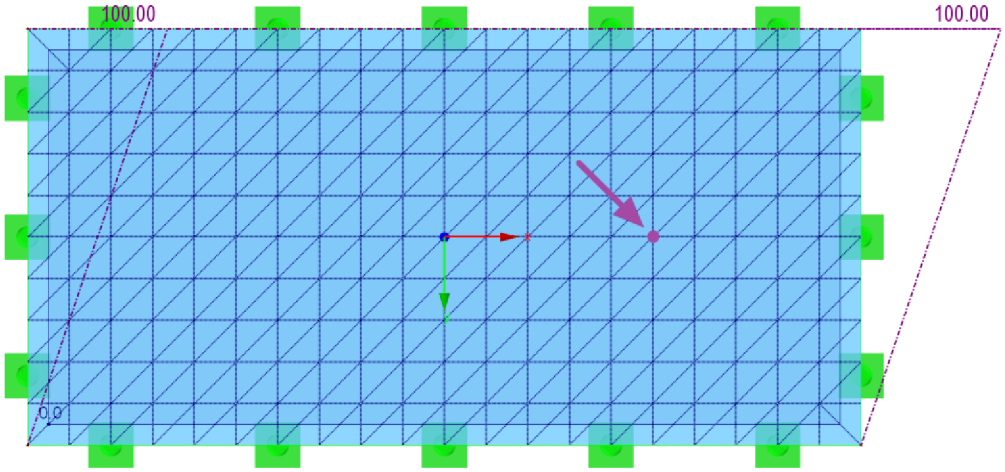

Fig. 26 Rectangular Membrane, FE Mesh, Local Cartesian Coordinate System Orientation, Imposed Deformation and Applied Perpendicular Forces, Node for Result Presentation (purple dot)

As there are different FE meshes during studying this example, it is not possible to focus on one particular element and instead, the results are presented in the particular grid point (the point for result presentation).

There are different mesh settings defined in the following table (Tab. 2). The results of the first principal force in the highlighted point are presented in the graph below (Fig. 26).

Tab. 2 Description of Eight Performed Analyses FE Data

Analysis number	1	2	3	4	5	6	7	8
FE size l_{FE} (mm)	500	400	300	200	100	50	25	12.5
Number of 2D FE	16	25	44	100	400	1600	6400	25600
Number of FE nodes	15	24	42	66	231	861	3321	13041
Equations number	45	72	126	198	693	2583	9963	39123

Four analyses were calculated for each FE mesh setting, since the imposed deformation was applied from left to right (right direction) and from right to left (left direction), and further both the wrinkling separation process (WS) and the shell with zero flexural stiffness (Shell) cases were also used.

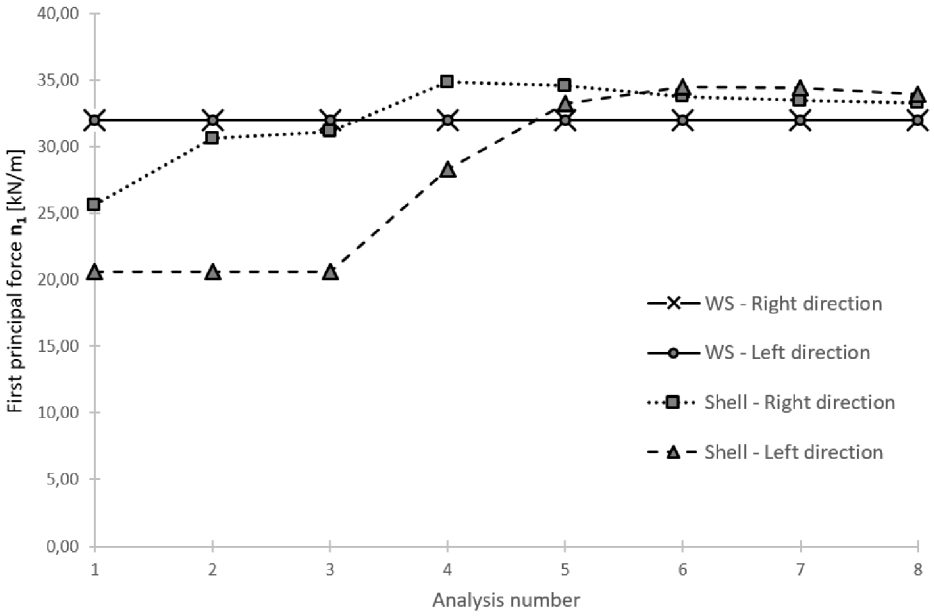

Fig. 27 Resulting Values of First Principal Force n_1 in Grid Point (Fig. 26) for Eight Different FE Refinements

Several conclusions can be made on the basis of the presented graph. First, the wrinkling separation procedure is independent of the mesh. Furthermore, when used the shell elements, a well-seen difference of the different imposed load direction is presented, which is the consequence of the alignment of the wrinkles with the FE mesh diagonals in the right direction, while the left direction causes the wrinkles which are crossing the diagonal direction (Fig. 26). However, both shell models converge to the results of the wrinkling separation procedure when the extensive refinement is used.

3.4.3 Shear Test of Rectangular Membrane for Isotropic Nonlinear Elastic and Plastic Material

The same geometry of the model and the imposed load conditions as in the previous example (Fig. 26) are now subjected to the analysis with the isotropic nonlinear elastic combined yielding criterion Von Mises/Rankine. The material properties are defined as $E = 900.0\ MPa, \nu = 0.45, t = 300.0\ \mu m$, the yielding stress $f_{y,t} = 21.0\ MPa$ and the elasticity modulus after yielding $E_p = 90.0\ MPa$.

An analogous comparison of the resulting values as presented in the previous example is made for the different mesh refinements (Tab. 2) and imposed load orientation. The example details and results are attached below (Fig. 28).

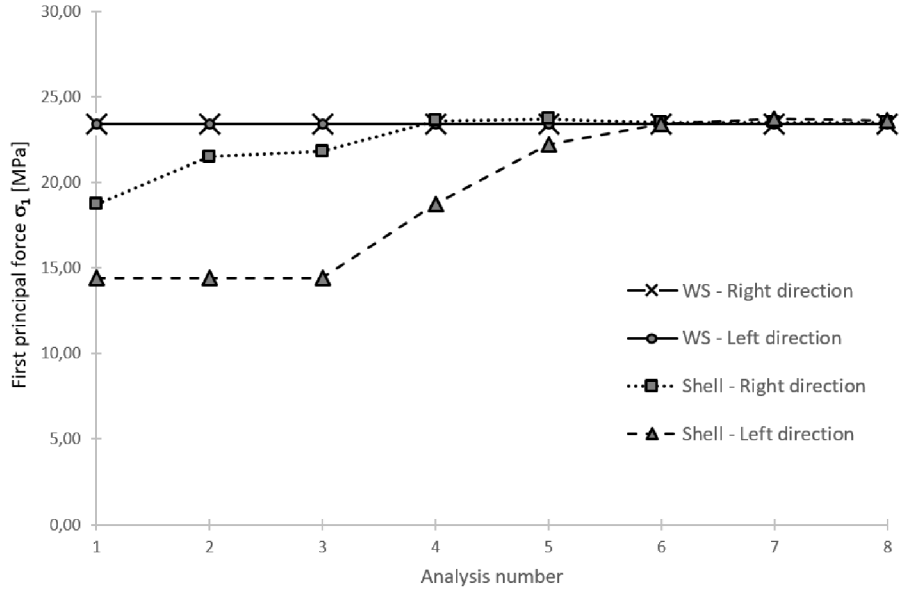

Fig. 28 Resulting Values of First Principal Force n_1 in Grid Point (Fig. 26) for Eight Performed Analyses

As well as in the previous example, when using the shell elements with the zero flexural stiffness, the diagonal directions have a considerable influence on the resulting stresses if the FE mesh is not refined enough. With the consequent decreasing of the FE length value, the shell solution converges to the wrinkling separation procedure solution, which is again independent of the mesh.

4 CUTTING PATTERN GENERATION

Due to the discrepancy between the double curvature of membrane structures and the planar pieces of the material they should be made of, the cutting pattern generation is an essential procedure to be performed before the manufacturing process. The quality of the generated patterns strongly affects the quality of the intended prestress approximation, thus this analysis precision is of a high importance.

The whole procedure could be divided into two essential steps. First, it is necessary to cut the spatial shape into appropriately sized pieces, therefore the spatial patterns are obtained.

The second task to be done is the flattening procedure, thus the planar patterns have to be calculated for their spatial shapes. This is inevitably connected with the necessary distortions, which have to be undertaken. However, it is of the highest interest to come with a procedure, which decreases this discrepancy as much as possible.

In addition to the engineering aspect of this task, the aesthetic importance of cutting patterns has to be considered as well, since the welding lines are a well-visible architectural element (Fig. 29).

Fig. 29 Shopping Centre Chodov in Prague (East Exit from Metro), Czech Republic [VI]

4.1 CUTTING LINES

Although a membrane surface could be generally divided into pieces by the arbitrarily chosen lines, two commonly used line types could be practically met there, namely the geodesic lines and the planar sections. The planar sections are created by the intersection of the definition plane with the membrane surface and sometimes, they are preferred. However, the geodesic lines are the most broadly used way when cutting double-curved surfaces, since they have considerable advantages arising from their nature as they lead to relatively straight planar patterns.

4.2 FLATTENING PROCEDURE

After dividing the surface into a series of spatial patterns, the flattening procedure is to be performed. Essentially, two different classes of this approximative task can be followed: the mathematical solution and the continuum mechanics solution procedures.

Following the physical class of methods, the flattening procedure is derived from the continuum mechanics basis. The pattern shape transformation from the space into the plane causes strains, and thus, searching for equilibrium is performed (Fig. 30).

$$\int_{{}^{t}V} {}_{t}\mathbf{C}\ {}_{t}\boldsymbol{\varepsilon}\ \delta_{t}\boldsymbol{\varepsilon}\ {}^{t}dV + \int_{{}^{t}V} {}^{t}\boldsymbol{\sigma}\ \delta_{t}\boldsymbol{\eta}\ {}^{t}dV = {}^{t+\Delta t}\boldsymbol{\mathcal{R}} - \int_{{}^{t}V} {}^{t}\boldsymbol{\sigma}\ \delta_{t}\boldsymbol{\varepsilon}\ {}^{t}dV \tag{4.1}$$

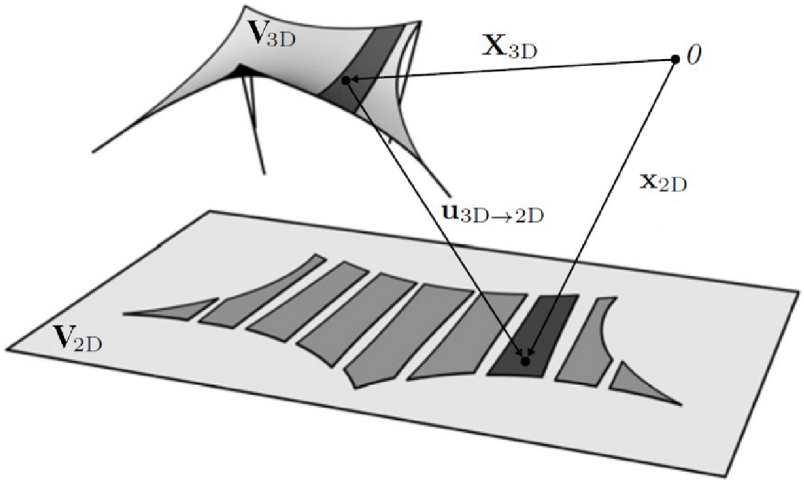

Fig. 30 Flattening Process ([9] with Modifications)

4.3 SPECIAL REQUIREMENTS FOR FLATTENING PROCEDURE

Even though the physical flattening procedure could be classified as a special case of FEA, there are some peculiarities and differences, which have to be satisfied during this analysis.

4.3.1 Orthotropic Directions

The local Cartesian axial system of the FE in the pattern has to be driven by its definition in the resulting pattern, not by the deformation of the FE axial directions in the space. In other words, the orthotropic directions have to be treated carefully while calculating the patterns to avoid violating the flattening process as well as the physical nature of the materials used.

4.3.2 Compatibility of Seam Lines

While the previous requirement was of physical nature, the other one is more the manufacturing restriction. The same length of the seam lines of the adjacent patterns is a required restriction during the flattening procedure $\Delta L_i = 0$ (Fig. 31).

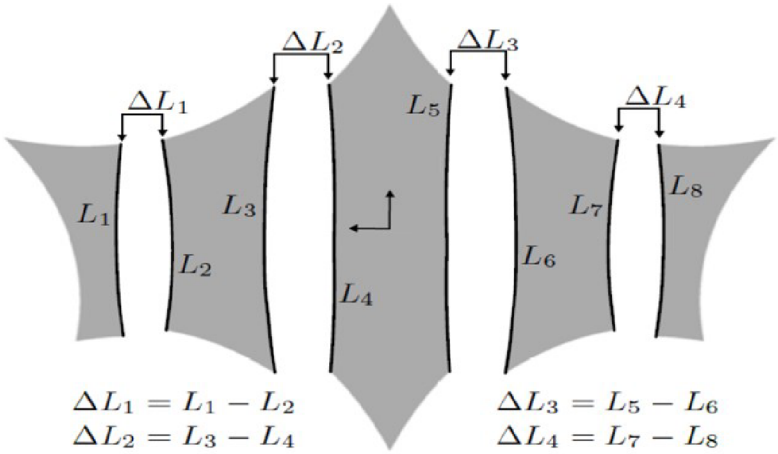

Fig. 31 Ensuring Same Lengths of Boundary Lines of Adjacent Patterns ([9] with Modifications)

4.3.3 Compensation

As the cutting pattern analysis deals with the membrane structures under pretension, the process of stress releasing has to be satisfied. Thus, the final pattern size is adjusted to satisfy the required pretension in the tensioned state. However, the woven fabric exhibits a nonlinear material response. Therefore, not only the form found shape with the required prestress has to be taken into account, but also the stresses reached in the nonlinear structural analysis. The goal of the applied compensation is to satisfy the approximation of the intended prestress after undergoing the loading cycles.

4.4 SELECTED CALCULATION PROCEDURES

For the development of the flattening procedure, the combination of the mathematical squashing (for estimating the shape in the first iteration) and the subsequent minimization of the energy differences sum was followed, as this process

provides the optimum combination of the speed and precision with the possibility of applying the selected material definition, structural requirements, etc.

4.5 EXAMPLES

The examples presented below demonstrate the usage of different cutting lines, the influence of the selected material during the flattening procedure, and the example dealing with the evaluation of the pattern quality [11].

4.5.1 Comparison of Usage of Different Cutting Lines

The example to be presented here is a hypar-shaped membrane structure. For splitting this model, different cutting lines are applied to demonstrate their influence on the resulting pattern shape. The prestressed spatial configuration is presented in the first figure (Fig. 32) and the shapes of the resulting patterns are shown in the second figure (Fig. 33).

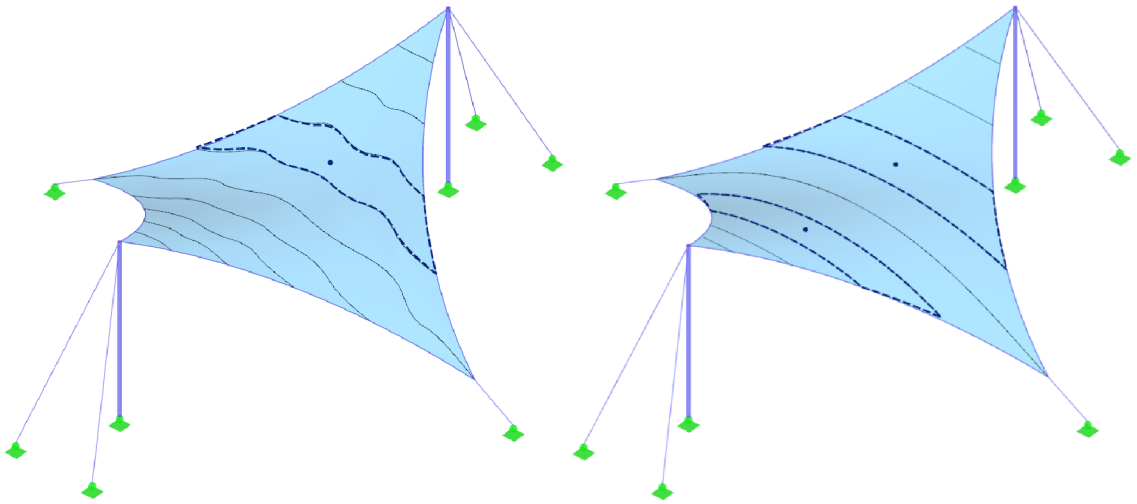

Fig. 32 Different Cutting Lines Used to Split Membrane: Irregular Lines (Left Pattern), Geodesic Lines (Middle Pattern) and Planar Sections (Right Pattern) [11]

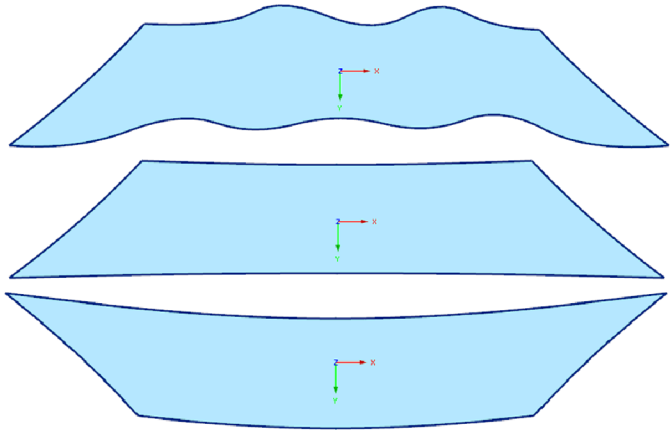

Fig. 33 Planar Patterns: Usage of Irregular Lines (Upper Pattern), Geodesic Lines (Middle Pattern) and Planar Sections (Lower Pattern) [11]

4.5.2 Evaluation of Flattened Patterns

The following structure is now analysed by using different cutting pattern layout definitions (Fig. 34, Fig. 35). In the first case, the membrane is divided into three patterns, and in the second case, it is divided into six patterns. The orthotropic material is used $E_x = 2000.0\,kN/m, E_y = 1000.0\,kN/m, G = 200.0\,kN/m, \nu_{xy} = 0.20, t = 1.00\,mm$.

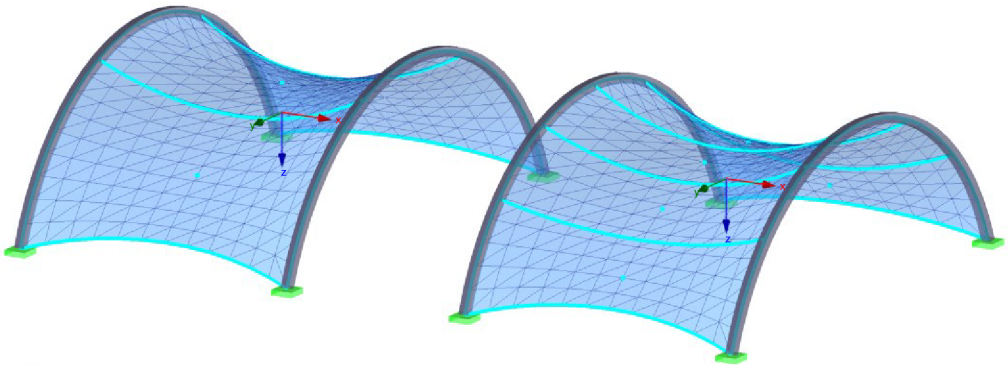

Fig. 34 Different Cutting Pattern Layouts and Orthotropic Directions Definition

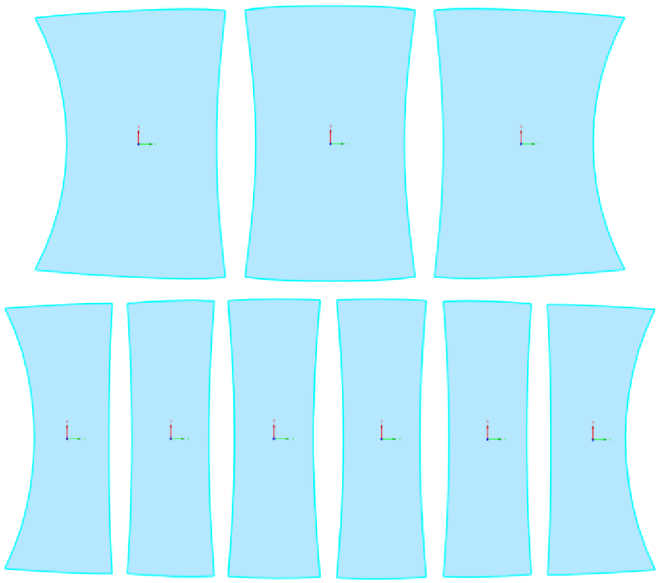

Fig. 35 Different Cutting Patterns Layouts After Flattening

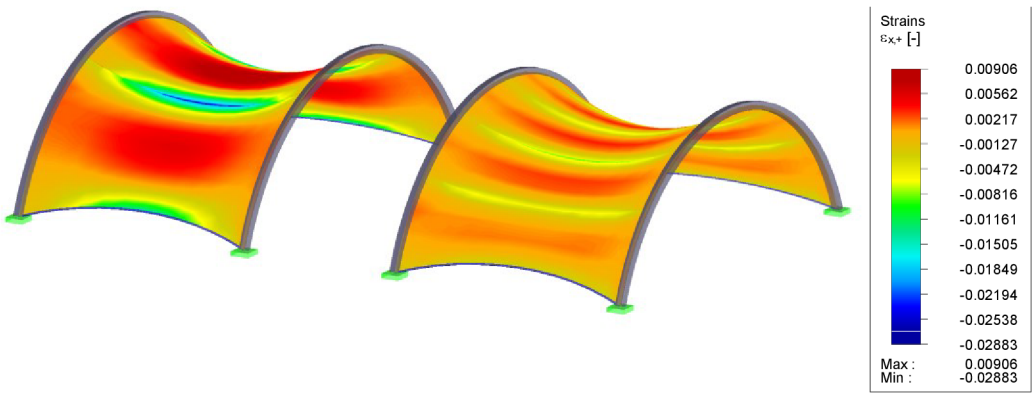

Fig. 36 Axial Strains ε_x

The selected layout has a considerable influence on the strains necessary for reaching the flat configuration (Fig. 36). By means of these results, it can be evaluated whether the pattern is suitable or not. Of course, the smaller are the patterns, the lower are the strains. But the manufacturing process, the aesthetic appearance and the available material widths should be considered as well. The results of the cutting pattern analysis can thus help when deciding for a pattern layout and the evaluation of their quality.

4.5.3 Examples of Complex Structure Patterning

The previous structures had quite simple configurations as they were intended to focus on particular tasks. The structure below, on the other hand, has the demonstrative purpose to show the pattern layout for a more complex membrane structure (Fig. 37, Fig. 38).

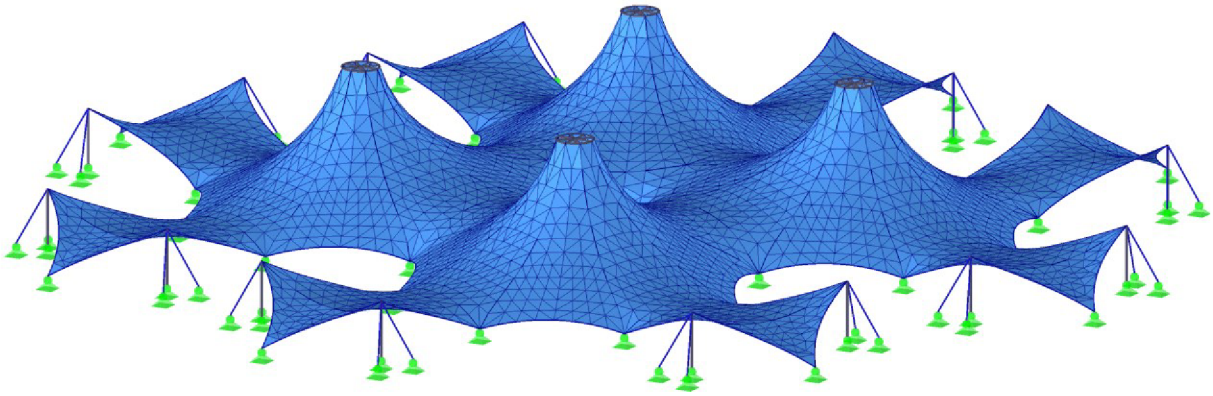

Fig. 37 Composition of Conical and Hypar Membranes

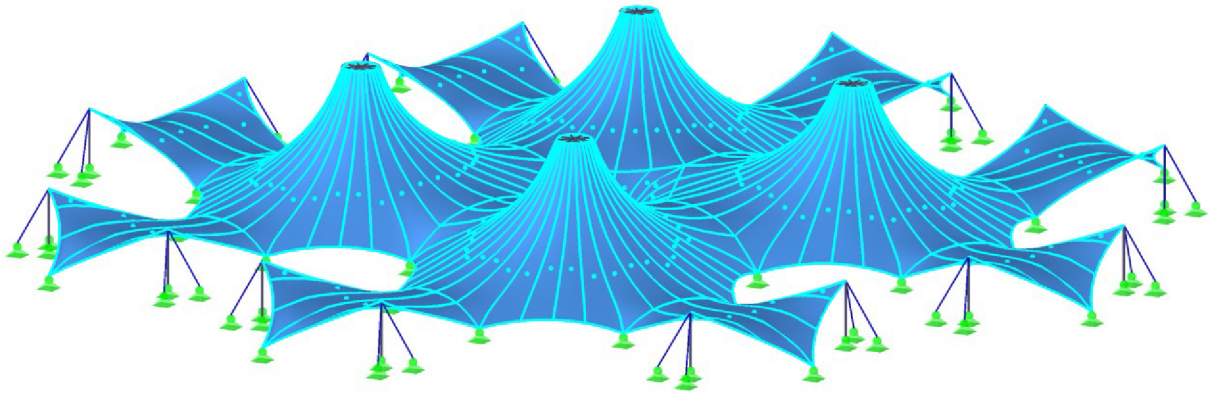

Fig. 38 Pattern Layout

5 USE IN PRACTICE

Due to the possibility of the fruitful interconnection of the research work performed in the academic environment and the development work performed in the established software companies, the calculation tools for membrane structures were developed in the framework of a teamwork and implemented into the RFEM software [III]. The calculation procedures are implemented as described above.

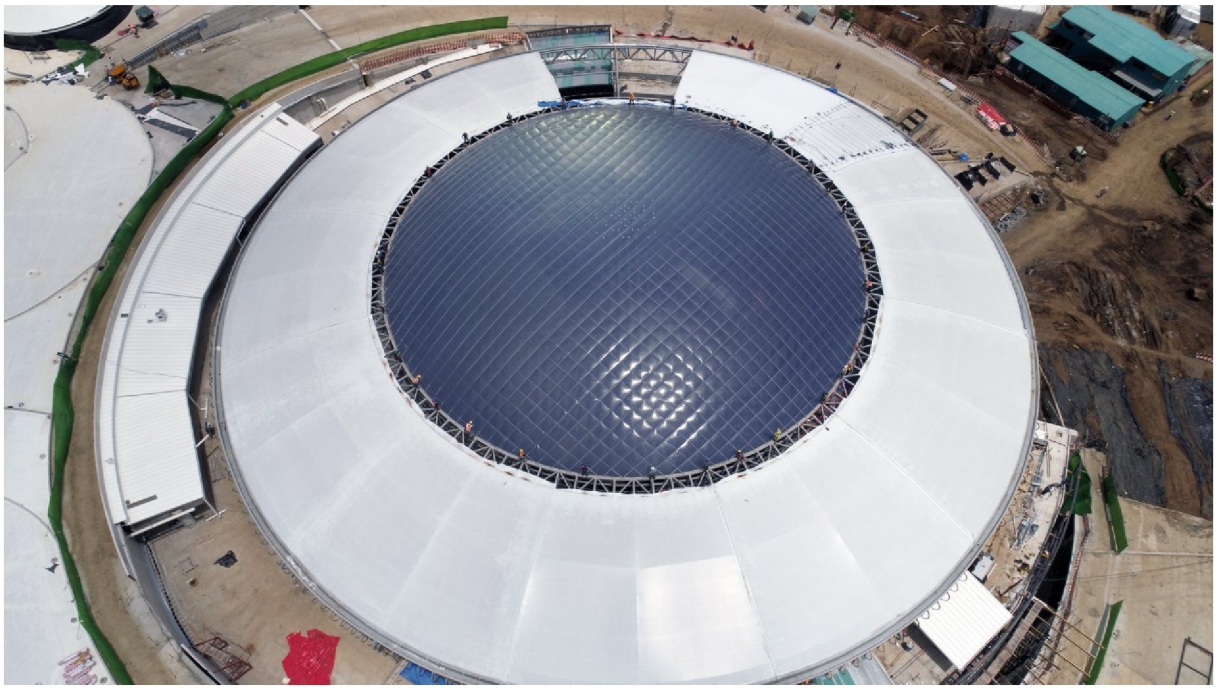

Fig. 39 Oxigeno in San Francisco de Heredia, San José, Costa Rica [VII]

Fig. 40 Interior View of Project Oxigeno, San Francisco de Heredia, San José, Costa Rica [VII]

USE IN PRACTICE

There is a really interesting customer project calculated by using the algorithms described above. This project's name is Oxigeno and it is located in San José, Costa Rica (Fig. 39, Fig. 40, Fig. 41). The detailed description could be found on the website [VII], where it is also stated: *'The ETFE cushion is the first one in the city of San Francisco de Heredia and at the same time the biggest in the world.'*

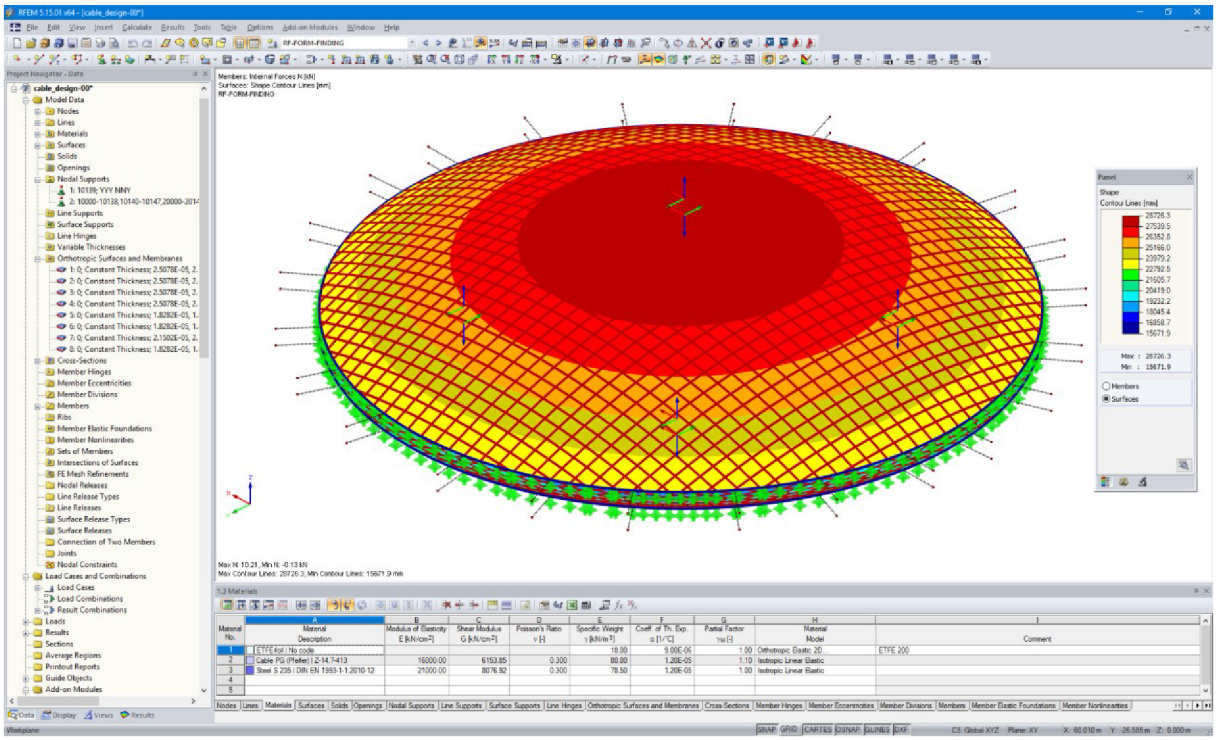

Fig. 41 Numerical Model of Project Oxigeno, San Francisco de Heredia, San José, Costa Rica [VII]

6 CONCLUDING REMARKS

Membrane structures are a really special kind of structures requiring uncommon designing steps in comparison with the conventional structures. The form finding procedure has to be performed at the beginning of the design process and cutting patterns need to be generated for the manufacturing process. For a proper structural analysis, it is also necessary to consider the wrinkling phenomenon, as the classic membrane theory does not ensure the real stress state estimation.

Each of the stated physical procedures were a part of the presented dissertation, thus the deep investigation of the current state of the art was carried out. Based on these investigations, the theoretical descriptions were written down at the beginnings of the particular chapter. Furthermore, the general and efficient methodologies selected for the numerical analysis were described. Also, the methods and calculation sequences proposed during the research work were presented. The whole work was supported by the beneficial interconnection of the research work at the university and the development work for the above-stated software companies. Thus, the theoretical sections, statements and proposals are followed by the results of numerical analyses that are demonstrating and proving the individual statements.

Based on the investigations performed in the field of the form finding analysis, the selected calculation procedure is derived from the ***geometric stiffness*** and ***hybrid*** platforms. Nevertheless, the crucial point of the form finding analysis consists of the equilibrium searching process itself. The necessity of reaching such a prestress is the cause of many different stabilization techniques. The advanced ***projection method*** was proposed for conical membranes, deriving the spatial equilibrium, which would not be possible to define directly, from the equilibrium in the arbitrary oriented projection plane, where it can be defined directly. This strong stabilization technique is quite unique in the principle, since it does not work as an emergency brake of an unrealistic prestress requirement as the stabilization techniques usually work, but it defines the exact equilibrium, although in the implicit manner. During the work focused on the form finding of tensile structures, the attention, was paid to the shape optimization procedure of the structures under compression or even of the structures with the mixed form finding requirements, in addition to the given scope of the dissertation thesis focus. The ***pushing method*** stabilization technique was proposed within the framework of the doctoral thesis to deal with these difficult and complex physical requirements. The above-described calculation procedures and the individual phenomena as well as the crucial implementation necessities were demonstrated on

particular examples. Namely, the independence of the equilibrium shape on the chosen initial approximation if the equilibrium of the forces within the given boundary conditions is known, the regeneration of the local axial system, the interaction of the supporting structure with the parts with shape analysing, presenting the result of the *projection method* and the *pushing method* stabilization techniques, or even the extraordinary phenomenon of the multiple equilibrium existence possibility for the structures with the mixed shaping requirements, etc.

Based on the investigations in the field of the wrinkling phenomenon, the new advanced and modular technique was proposed. The process of dealing with the linear elastic materials was named ***wrinkling separation***, while the procedure of dealing with the nonlinear elastic or plastic materials was named ***elastic prediction modification***, which incorporates the *wrinkling separation* algorithms inside as a modular part. These procedures separate out the unnatural stress, which would be considered by the standard membrane theory, but cannot appear in the membrane as a consequence of its physical nature. Furthermore, the proposed methods were extensively verified, and few of the analyzed examples were incorporated into this work to prove their reliability. The first benchmark example disposes with the analytical solution, while the other examples use the well-known equivalency of the wrinkling models with the extensively refined discretization in combination with the shell elements with zero flexural stiffness.

In the chapter focused on the generation procedure of cutting patterns, the possible approaches were presented, and both their advantages and disadvantages were mentioned. Based on the deep investigations performed in this research area, the ***optimum algorithmic sequence*** was proposed to combine the strengths of the individual methods. As the ***mathematical squashing*** is a really good initial approximation for the planar patterns, the pattern shapes obtained in this way were consequently used for the advanced ***minimization of the energy differences*** between the spatial and the planar patterns. This combination thus exhibits an increasing calculation performance while ensuring the physically optimized patterns. At the end of this section, the numerical examples proved particular statements mentioned in this section, and they demonstrated the possibility of the resulting pattern quality evaluation.

The fascinating field of tensile structures attracts the attention of many researchers and developers as there is still a huge space for further investigations and improvements. Among others, for example, the automatic compensation of patterns, which has to be derived from the intended prestress and inelastic strains, undergone

an evolution during the lifetime. Thus, not only the form finding results, but also the static analysis results have to be the basis of this process. Some authors performed the analyses of the mounting process simulation by tensioning the planar patterns into their final form, as this analysis allows for getting closer to the real stress state of the erected structures. Here, the mutual interaction of all the processes could be observed since the form finding affects the structural behaviour, and the shape to be patterned, the structural analysis influences, the necessary compensation, and the reassembly process lead to a closer approximation of the erected structure, but also affects the structural analysis response itself. Thus, the investigation of the proper analysis sequences and impacts is of a great interest and will be a part of a future work in the field of membrane structures.

7 REFERENCES

1 Argyris, J.H., Angelopoulos, T., & Bichat, B. (1974). A general method for the shape finding of lightweight tension structures. *Computer Methods in Applied Mechanics and Engineering*, 3(1), 135-149.

2 Tabarrok, B., & Qin, Z. (1992). Nonlinear analysis of tension structures. *Computers and Structures*, 45(5–6), 973-984.

3 Barnes, M.R. (1999). Form Finding and Analysis of Tension Structures by Dynamic Relaxation. *International Journal of Space Structures*, 14(2), 89-104.

4 Linkwitz, K., & Schek, H.J. (1971). Einige Bemerkungen zur Berechnung von vorgespannten Seilnetzkonstruktionen. *Ingenieur-Archiv*, 40(3), 145-158.

5 Schek, H.J. (1974). The force density method for form finding and computation of general networks. *Computer Methods in Applied Mechanics and Engineering*, 3(1), 115-134.

6 Haber, R.B., & Abel, J.F. (1982). Initial equilibrium solution methods for cable reinforced membranes part I—formulations. *Computer Methods in Applied Mechanics and Engineering*, 30(3), 263-284.

7 Bletzinger, K.U., & Ramm, E. (1999). A General Finite Element Approach to the Form Finding of Tensile Structures by the Updated Reference Strategy. *International Journal of Space Structures*, 14(2), 131-145.

8 Veenendaal, D., & Block, P. (2012). An overview and comparison of structural form finding methods for general networks. *International Journal of Solids and Structures*, 49(16), 3741–3753.

9 Dierigner, F.H. (2014). *Numerical Methods for the Design and Analysis of Tensile Structures.* Dissertation, München: Technische Universität München.

10 Jrusjrungkiat, A. (2009). *Nonlinear Analysis of PneumaticMembranes: "From Subgrid to Interface".* Dissertation, München: Technische Universität München.

11 Lang, R. (2017). *Design and Analysis of Membrane Structures in FEM-Based Software.* Diploma thesis, Dessau-Roßlau: Anhalt University of Applied Sciences.

12 Akita, T., Nakashino, K., Natori, M.C., & Park, K.C. (2007). A simple computer implementation of membrane wrinkle behaviour via a projection technique. *International Journal for Numerical Methods in Engineering*, 71, 1231–1259.

13 Stein, M., & Hedgepeth, J.M. (1961). *Analysis of partly wrinkled membranes.* NASA TN D-813.

8 LIST OF PUBLISHED WORKS

14 Lang, R., Němec, I., Hokeš, F., & Trcala, M. (2019). Different Sources of Dynamic Damping and Nonlinear Dynamic Analysis of the Membrane Construction. *First International Nonlinear Dynamics Conference, NODYCON 2019.*

15 Lang, R., & Němec, I. (2017). Form-finding of shell and membrane structures. *International Conference on Textile Composites and Inflatable Structures, STRUCTURAL MEMBRANES 2017.*

16 Hofírek, R., Lang, R., & Zich, M. (2017). Changes in shrinkage after the application of insulation to the concrete surface. *Solid State Phenomena*, 272, 121-126.

17 Hofírek, R., Lang, R., & Zich, M. (2017). Změny průběhu smršťování po aplikování izolace na povrch betonu. *24. Betonářské dny 2017.*

18 Lang, R., Němec, I., & Štekbauer, H. (2017). Navrhování tvarů membránových konstrukcí a výpočet střihových vzorů. *TZB-info*, 2017.

19 Lang, R., Zeiner, M., & Němec, I. (2016). Vytváření střihových vzorů. *Juniorstav 2016.*

20 Lang, R., & Němec, I. (2015). Jak navrhovat membránové konstrukce. *Juniorstav 2015.*

21 Lang, R., Němec, I., & Martinásek, J. (2014). Specifické aspekty ohybově netuhých konstrukcí. *12th International Conference on New Trends in Statics and Dynamics of Buildings.*

22 Lang, R., Němec, I., & Ševčík, I. (2014). Form- finding of membrane structures with regard to its specific necessities. *6th international conference Dynamics of Civil Engineering and Transport Structures and Wind Engineering, DYN-WIND 2014.*

23 Lang, R., Němec, I., & Ševčík, I. (2014). Form-finding of Membrane Structures and Necessary Stabilization of this Process. *Applied Mechanics and Materials*, 617, 130-135.

24 Němec, I., & Lang, R. (2013). Design and analysis of the membrane structure of a stadium roof. *Applied Mechanics 2013.*

25 Lang, R., & Němec, I. (2013). Navrhování membránových konstrukcí. *Modelování v mechanice 2013.*

26 Němec, I., & Lang, R. (2013). Návrh počátečního tvaru pro membránové konstrukce. *Sborník vědeckých prací Vysoké školy báňské – Technické univerzity Ostrava*, 2, 159-162.

9 LINKS

I Wikipedia (2019). Retrieved 7 July 2019, from https://de.wikipedia.org/wiki/Tanzbrunnen

II Tanzbrunnen Köln (2019). Retrieved 7 July 2019, from https://www.koelnkongress.de/en/locations/tanzbrunnen-koeln.html

III Dlubal Software – Structural Engineering Software for Analysis and Desing (2019). Retrieved 7 July 2019, from https://www.dlubal.com/en-US/solutions/industries/analysis-and-design-software-for-tensile-membrane-structures

IV FEM consulting – Research and development of FEM solver (2019). Retrieved 7 July 2019, from http://www.fem.cz/?lang=en

V Architen Landrell (2019). Retrieved 7 July 2019, from http://www.architen.com/articles/basic-theories-of-tensile-membrane-architecture/

VI Archtex (2019). Retrieved 7 July 2019, from http://archtex.cz/en/index.html

VII Dlubal Software – Structural Engineering Software for Analysis and Desing – Customer Projects (2019). Retrieved 19 August 2019, from https://www.dlubal.com/en/downloads-and-information/references/customer-projects/001116

10 About author

Personal Information

Rostislav Lang
Institute of Structural Mechanics
Faculty of Civil Engineering
Brno University of Technology
Veveří 95, 635 00 Brno
Email: lang.r@fce.vutbr.cz

Education

From 2013 Student of Doctoral Programme in Civil Engineering EQF 8
Brno University of Technology, Faculty of Civil Engineering
Brno, Czech Republic

- Degree course: Structures and Traffic Constructions
- Doctorate thesis: Algorithms for design and analysis of membrane structures

2015 - 2017 Master Programme in Civil Engineering EQF 7
Anhalt University of Applied Sciences, Institute for Membrane and Shell Technologies e.V.
Dessau-Roßlau, Germany

- Degree course: Membrane Strucutures
- Master thesis: Design and Analysis of Membrane Structures in FEM-Based Software

2011 - 2013 Master Programme in Civil Engineering EQF 7
Brno University of Technology, Faculty of Civil Engineering
Brno, Czech Republic

- Degree course: Structures and Traffic Constructions
- Master thesis: Design and Analysis of Membrane Roof of a Stadium

2007-2011 Bachelor Programme in Civil Engineering EQF 6

Brno University of Technology, Faculty of Civil Engineering

Brno, Czech Republic

- Degree course: Structures and Traffic Constructions
- Bachelor thesis: The Girder Bridge Analysis

WORK EXPERIENCE

From 10/2016 Tutor

Brno University of Technology, Faculty of Civil Engineering, Institute of Structural Mechanics

Veveří 331/95, 602 00 Brno, Czech Republic

- Courses

BD003	Structural Analysis 1
BD004	Structural Analysis 2
CD002	Nonlinear Mechanics

From 4/2014 Research fellow

FEM consulting s.r.o.

Veveří 331/95, 602 00 Brno, Czech Republic

- Professional and organizational responsibility for algorithmization of calculation tools for the design and analysis of membrane structures within the FEA core by FEM consulting company
- Implementation of form finding algorithms, physical flattening process and wrinkling of membranes into the FEA core
- Responsible for cooperation with the partner company Dlubal Software for development of software packages for membrane structures into RFEM software (RF-FORM-FINDING and RF-CUTTING-PATTERN)

4/2013 – 3/2014 Software development analyst

Dlubal Software s.r.o.

Anglická 28, 120 00 Praha 2, Czech Republic

- Organizational and analytic work for development of calculation modules for membrane structures into RFEM software

2/2013 – 3/2013 Design works and projects

HURYTA s.r.o.

Staňkova 557/18a, 602 00 Brno, Czech Republic

- design and calculation of building structures

6/2012 Diagnostics of constructions / professional experience during study

INSET s.r.o.

Vinohrady 506/40, 639 00 Brno, Czech Republic

- instrumental works during static and dynamic load tests of highway bridges

PARTICIPATION IN RESEARCH PROJECTS

1/2016 – 12/2018 CZ.01.1.02/0.0/0.0/15_019/0004929

Algorithmization of the initial shape design of the membrane structures and their static and dynamic analysis

1/2015 – 12/2015 FAST-J-15-2803

Design of membrane structures

3/2014 – 06/2015 CZ.1.03/2.2.00/23.00705

Development of progressive methods in solid mechanics

1/2014 – 12/2014 FAST-J-14-2351

Design of initial equilibrium shape of membrane structures (form finding)

AWARDS

2015 Award of Josef Hlávka received from the Foundation 'Talent of Josef, Marie and Zdenka Hlavka'

2015 17th International Conference of Postgraduate Students JUNIORSTAV 2015: Diploma for the 1. place in section 2.7 Structural mechanics and diploma for the best paper of the conference

2013 Award for academic achievement received from the dean of the Faculty of Civil Engineering, Brno University of Technology

2013 Award for diploma thesis received from the dean of the Faculty of Civil Engineering, Brno University of Technology

2013 Third place in the theses competition in the degree course Structures and Traffic Constructions. Note: Competition was organized by ČKAIT (Czech chamber of engineers and technicians active in construction) and Brno University of Technology, Faculty of Civil Engineering.